

Emissions Reduction Technologies for Military Gas Turbine Engines

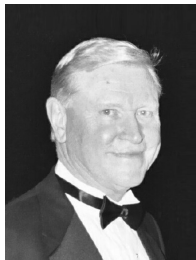
G. J. Sturgess

Innovative Scientific Solutions, Inc., Dayton, Ohio 45440-3638

and

Joseph Zelina, Dale T. Shouse, and W. M. Roquemore

U.S. Air Force Research Laboratory, Wright–Patterson Air Force Base, Ohio 45433-7251



Geoffrey Sturgess is a founding member of Innovative Scientific Solutions, Inc. (ISSI), and has been in Dayton with ISSI for the last eight years. Before ISSI, he spent 23 years with Pratt and Whitney in East Hartford, Connecticut, and also worked at Parker-Hannifin in Cleveland, Ohio, and the Aircraft Engine Group of General Electric (GE) in Lynn, Massachusetts. He was recruited by GE in 1968 from England, where he was a research fellow on the faculty of Loughborough University after spending time with Rolls–Royce, plc., in both Bristol and Coventry, England, U.K. G. Sturgess was educated at Loughborough University, Loughborough, England, U.K., and Imperial College of Science and Technology, London. He currently lives in Maine, on beautiful Casco Bay. Sturgess is a Fellow of AIAA and has over 80 publications.



Joseph Zelina received his Ph.D. from the University of Dayton in 1995, where he conducted research at the U.S. Air Force Research Laboratory studying combustion processes and pollutant emission formation. He spent nearly six years at Honeywell Engines and Systems, formerly Allied Signal Engines, as principal engineer in the Combustion and Emissions Advanced Technology Group, where he was principal investigator for the NASA Advanced Subsonic Technology, NASA Ultra Efficient Engine Technology, and Department of Defense Joint Turbine Advanced Gas Generator combustor programs, and was principal investigator and program manager for several internally-funded research and development efforts including fuel injector coking, fuel spray laser diagnostics, and low-emissions combustor design programs. He has two patents and two patents pending on combustion system designs. Three years ago, he joined the U.S. Air Force Research Laboratory, Combustion Branch, as a senior combustion research engineer, where he leads the Ultra-Compact Combustor/Inter-Turbine Burner Research Program. J. Zelina is a Senior Member of AIAA.



Dale Shouse is a senior combustion research engineer in the Combustion Science Branch of the Turbine Engine Division. He is the director for in-house research and development activities for advanced military aircraft combustion systems. He participates on several integrated product teams and consults with various industry, university, and other government organizations on gas turbine combustion and augmentor programs. D. Shouse has 23 years experience in gas turbine engine research and development. He has a B.S. degree in mechanical engineering from the University of Dayton. He has published 29 technical papers including 5 journal articles and has received recognition for Best Applications Paper for Combustion and Fuels (1994 and 2001). D. Shouse has been the recipient of several U.S. Air Force Propulsion Directorate Awards for Engineer of the Year as well as the H. D. Heron Award. He holds several patents including one for the “Trapped Vortex Combustor.”



William M. (Mel) Roquemore serves as senior research scientist and independent researcher in the field of airbreathing combustion, diagnostics, and fuels technologies. He conceives, plans, and advocates major research and development activities; consults with the director of propulsion, division chiefs, and staff concerning the total reach program and results; monitors and guides the quality of scientific and technical resources; and provides expert technical consultation to other U.S. Air Force organizations, Department of Defense, and government agencies, universities, and industry. W. Roquemore entered federal service in 1963 and held a variety of technical leadership positions in airbreathing propulsion. He was appointed senior scientist, Combustion, in 2000. He is a Fellow of AIAA.

Future military gas turbine engines will have higher performance than current engines, resulting in increased compressor and combustor exit temperatures, combustor pressures, and fuel-air ratios with wider operating limits. These combustor characteristics suggest undesirable exhaust emission levels of nitrogen oxides and smoke at maximum power and higher carbon monoxide and unburned hydrocarbons at low power. To control emission levels while improving performance, durability and cost, requires major advances in combustor technology. Current emissions control approaches as applied to conventional swirl-stabilized combustors include rich- and lean-burn strategies, together with staged combustion. These approaches, even in fully developed form, may not be sufficient to satisfy the projected design requirements. Unconventional combustor configurations may become necessary. Different engine cycles other than the standard Brayton cycle may also be used for special applications in order to avoid the use of excessive combustion temperatures. The paper presents an overview of the currently utilized emissions control approaches, comparing their performances and likely potential for meeting future requirements. Experimental results are presented for two non-conventional combustor configurations that have shown promise for advanced engine applications. A brief discussion is offered on cycle changes that could result in lower peak temperatures while maintaining advanced performance.

Introduction

GLOBAL warming tends to excite the media and the public, via input from the various environmental groups. Global warming is, in fact, a major issue and is generally interpreted as extreme greenhouse warming of the atmosphere that leads eventually and progressively to catastrophic environmental consequences. Trace gases in the atmosphere play an important role in atmospheric equilibrium. They absorb infrared and ultraviolet radiation. The stored radiative energy increases the atmospheric temperature, which then influences the surface conditions. Because the trace gases are traces, their concentrations are easily changed by relatively small perturbations. Naturally occurring trace gases, which are also known as greenhouse gases because of their behavior, are carbon dioxide CO_2 , methane CH_4 , nitrous oxide N_2O , and water vapor H_2O . These gases are all increasing in the atmosphere. Industrial activity from fossil fuel burning is an undoubted contributor to these increases. Some of the introduced trace gases chemically affect the base-level trace gases through photo-chemical activity. The greenhouse effect, based on well-understood scientific principles, was predicted by Arrhenius (1859–1927) at the beginning of the 20th century. The role of industrial activity in global warming is highly controversial. Total human production of CO_2 is about 6 gigaton of carbon equivalent per year, and this is but a small fraction of the total exchanges of CO_2 occurring naturally each year between the oceans and the atmosphere, between vegetation and the atmosphere, and within the ocean itself and its biota. The observed rise in atmospheric CO_2 amounts to about one-half that of the estimated amount released due to total industrial activity. Nonetheless, CO_2 from industrial activity does contribute to the process. It is well-known that global temperatures are historically not constant. The Earth has been in a consistent warming trend since the end of the little ice age, 300 years ago, which predates the industrial revolution by 100 years. Northern hemisphere temperatures (a rolling 11-year average) since the little ice age correlate very well with the solar magnetic cycle length: The shorter the magnetic cycle, the more active and, hence, brighter the sun is.¹ The current length of the cycle is about 20–22 years. The radius of the sun also fluctuates sinusoidally with about an 80–100 year period. The solar variations observed are consistent and typical for stars similar in age and mass to the sun. The solar constant is in actuality, not a constant at all. The observed increases in atmospheric CO_2 during this period are entirely consistent with the oceans giving off dissolved gases as their temperatures increase. Therefore, although fossil fuel burning contributes to global warming, to an unknown but perhaps significant degree, it does not appear to be the root cause.

Each kilogram of jet fuel burned produces, on average, about 3.2 kg of CO_2 . Aviation is responsible for only 2 or 3% of the total due to human industrial activity. The best way to reduce CO_2 produced by aircraft is for aircraft to burn less fuel. Improvements in aircraft productivity and aerodynamic design, and in engine design, have reduced the fuel consumption per seat-kilometer for passenger aircraft by a factor of about 2.75 since the British Comet 1 introduced commercial jet transportation in the 1950s. Although the easy things have all been done, the downward trend in fuel consumption with

time is expected to continue, albeit at a reducing gradient. Therefore, CO_2 from aviation is not currently a prime concern given the natural levels in the Earth environment and its small contribution to the industrial activity total.

Transportation is responsible for most of the carbon monoxide CO, unburned hydrocarbons (UHCs), and oxides of nitrogen NOx introduced into the atmosphere through industrial activity. Although the aircraft contributions to the total transportation emissions of these pollutants are only very small (around 1%), unfortunately, they are concentrated at ground level around airfields and at altitude in well-defined flight corridors. The majority of the aircraft engine emissions are introduced into the 30–60° latitude band of the northern hemisphere, with the bulk of the emissions being introduced in the troposphere at 10–12 km altitude. Around airfields, these emissions contribute to smog formation; at altitude, there are a number of photochemical reactions taking place that have effects on the important trace gases. In addition, aviation fuels contain small quantities of sulphur (around 0.05% by mass) as impurities that are important contributors to fuel lubricity, which is very low. In the U.S. fuels the sulphur content has consistently increased over the last 20 years. At sea level, the sulphur appears in the engine exhaust as oxides of sulphur (SO_x that add to the smog issue); at altitude, based on airborne sampling by chase aircraft, the sulphur appears in the near-plume as sulphuric acid, H_2SO_4 (Refs. 2 and 3). There are clear indications that the resulting contrail formation, where the aerosols of H_2SO_4 /UHCs [or volatile organic compounds (VOCs)]/carbon particles found at high altitudes in persistent (3–18 h) aircraft exhaust plumes add substantially to the numbers of atmospheric microscopic particles. These serve as nucleation sites (10% increase in sites relative to out-of-plume) for water vapor and are affecting cirrus cloud formation along well-traveled flight corridors. The potential here is that increased cloud cover changes the Earth's albedo or reflectivity to solar radiation and, hence, affects atmospheric equilibrium.

The U.S. Environmental Protection Agency (EPA) has identified aircraft gas turbine engines as a significant emissions source and established regulations governing the emission of CO, UHCs, NOx, and smoke (47 Federal Register 58462). The EPA has amended the regulations by adopting the U.N. International Civil Aviation Organization (ICAO) regulations for CO and NOx (62 Federal Register 89). The amended regulations apply to commercial aircraft engines with rated thrust greater than 26.7 kN that are either newly certified or newly manufactured after 7 July 1997. The limits for gaseous emissions are expressed as integrated values around a defined landing and takeoff cycle for an engine operating at sea level on a standard day and, thus, govern emissions below 900-m altitude. The unit of measure is grams of pollutant per kilonewton of rated thrust, and the allowable maximum values are specific numbers for CO and UHCs, and for NOx they are expressed as a function of engine compression ratio. NOx is reported as nitrogen dioxide NO_2 corrected to 0.0063-lbm H_2O /lbm air specific humidity. UHCs are reported as methane CH_4 . Smoke limits are expressed in terms of an Aerospace Recommended Practices (ARP) smoke number, as a function of rated thrust. Because production

engines of the same type exhibit a degree of variability in performance, and because there is measurement uncertainty and repeatability to contend with as well as different atmospheric background levels and conditions, statistical compliance levels have been established. Over the years the limiting values for NO_x have been progressively lowered, and this continues, for example, committee on aviation environmental protection (CAEP)/4 rule (2004), with CAEP/6 and CAEP/8 to follow. For a summary of the status, see Ref. 4. Discussion is taking place concerning regulation for exhaust emissions at altitude.⁵ Although the regulations existing govern operations below 900 m in altitude, they also result in some inherent reduced emissions capabilities at altitude although they may not be optimized for those conditions. Furthermore, there are growing concerns over the particulates, which can be solid and liquid phase (VOCs), and their sizes that are associated with smoke. For these reasons, emissions control has become a major design requirement for combustors intended for commercial aircraft engines.

Although U.S. military aircraft are exempt from the EPA emissions standards governing commercial aircraft, there is a legal requirement currently applicable to military airbases that can impact military aircraft emissions. All Department of Defense bases must comply with the National Ambient Air Quality Standards (NAAQS) and State Implementation plans. Specifically, the military must comply with the general conformity requirement described in Section 176(c)(1) of the Clean Air Act, as implemented by the EPA in the General Conformity Rule (GCR). This requires that when a federal agency is proposing a new activity in nonattainment or maintenance areas, the agency must assure that the activity conforms to the State Implementation Plan, which documents the schedule and how the state will bring the region into conformity with the NAAQS.

Basing of future military aircraft systems may require emissions reductions to avoid deployment issues in areas of nonattainment. For a military airbase to comply with the GCR, the military must evaluate all emissions of the nonattainment pollutant from new stationary and mobile sources, including aircraft operating below 3000 ft and ships where appropriate. If the total amount of criteria pollutants [ozone, CO, or particulate matter (PM)] or precursors of ozone such as NO_x and VOCs exceeds the EPA established minimum levels, the military must demonstrate how they will conform to the State Implementation Plan for the area. Typically, the emissions from aircraft dominate the emissions from an active military airbase. In this situation, an airbase in a nonattainment region can have difficulties in deploying new aircraft systems and even transferring aircraft from one base to another. Commercial airports as communities must also comply with the NAAQS, although commercial aircraft movements themselves are exempt from the NAAQS.

Almost all of the emissions reductions technology extant has been developed specifically for the commercial engine market. Furthermore, it has been directed toward satisfying the ICAO landing/takeoff cycle emissions standards. Although lists of design requirements for aircraft gas turbine engine combustors for commercial and military applications would appear to be superficially similar, the emphasis, priorities, and parameter-values assigned to those lists would be quite different between the two applications. For these reasons, the suitability of various emissions reduction strategies for military applications is not equal in all cases. Nevertheless, although commercial and military aircraft can also have very different mission profiles, they can share general emissions reduction technologies in principle, provided appropriate balances are obtained between emissions reductions and operability issues. However, any commercially developed emissions strategy that is considered for military use has to be very carefully reviewed against the way that military aircraft are operated by the war-fighter. Under gun-to-gun combat conditions, aircraft maneuverability is paramount, with rapid high-gee, high-incidence turns taking place over wide ranges of altitude and subsonic speeds, with associated rapid and extreme throttle movements being normal. The combustion equipment must be robust enough to keep functioning perfectly at these conditions.

There follows a broad, yet necessarily brief, description concerning the development of current emissions reduction technology, its capabilities and limitations, and some advanced techniques that might offer further reductions in exhaust emissions. For the sake of brevity, the discussion is confined to the gaseous emissions of CO, UHCs, and NO_x only, except for where trades involving smoke are concerned. In addition to brevity, a reason for this decision is that visible smoke reduction technology is generally well understood. The recent concern over very small particulates (PM_{2.5s}) that visible smoke reduction technologies tend to produce and that exist as solids, liquids, and solids with liquid coatings, and that do not readily settle from the atmosphere is worthy of a separate study, as some passing remarks in the text suggest. Furthermore, the standard filter paper used in the ARP 1179 smoke test does pass dry particulates up to 117 nm in equivalent diameter. Because emissions reductions technology is largely considered to be company proprietary, the work presented is necessarily confined to material available in the open literature. Discussion is also limited to efforts of the two U.S. large engine manufacturers. This is not to imply that other sources have not contributed to the knowledge base. Small engine manufacturers, in particular, have a difficult time with respect to low-emissions combustor equipment because of obvious size limitations and the strong cost driver that they must live with.

Important Tradeoffs

Tradeoff in the area of emissions control can involve two types of trading: first, trades between the different emissions and second, trades between emissions and combustor performance. Both types of trading have been conducted at times to achieve overall emissions compliance. Ideally, any emissions control strategy should represent a true emissions reduction, that is, a simultaneous reduction for all gaseous and particulate emissions. Given the conflicting nature of emissions generation mechanisms at low and high engine power levels, it can be very difficult to reduce always simultaneously all emissions. Therefore, it is common to employ some form of limited trading between emissions. Extreme emissions trades, for example, reducing NO_x to very low levels at the expense of vastly increased CO, are not usually acceptable. Of course, the major trend of reducing fuel consumption, and hence CO₂ emissions, has been achieved by increasing engine overall pressure ratio and peak temperature ratio, along with increasing bypass ratio. These cycle changes make the NO_x problem more difficult. Therefore, there is an implicit trade that exists in modern engine design between CO₂ and NO_x emissions. Although NO_x is perceived as being more important than CO₂ in aircraft emissions, of course, economics also play the dominant role in the drive for reduced fuel burn.

Any component design changes incorporated for reasons of achieving low emissions must allow the combustion system to still satisfy the basic design requirements. However, once basic minimums have been satisfied, there are usually adequate margins for trading some combustor performance for improved emissions, provided that engine requirements are met. For example, it is not necessary to always achieve combustor lean blowout fuel/air ratios that are, for example, as low as 1/10th the minimum fuel/air ratio that the engine will ever experience.

Governing Philosophy

As already above successful emissions control usually involves two kinds of compromise and is, therefore, challenging. It encompasses considerations of initial control concepts, sensitivity determinations, and optimization of both emissions and performance behaviors. These necessary steps have to be considered together and not in isolation. Optimization requires sufficient understanding of the underlying chemistry and physics to allow formulation of some working hypotheses that frequently have to be bounded by engineering pragmatism. One constraint that has to be rigidly applied at all times is that safety should never be compromised.

Reacting flow behavior in combustors is governed by an elliptic set of simultaneous, nonlinear, second-order partial differential equations. The potential behavior of such an equation set implies that the fine details of the flow are important. Fortunately, there is always sufficient generality at an engineering working level such that, with care, useful guidance can be obtained to make low-emissions approaches both possible and portable from engine-to-engine designs.

Control Approaches

Approaches to control emissions can be divided into two broad types: 1) those approaches that may be applied to conventional-appearing combustors and 2) those approaches that result in nonconventional-appearing combustors. Under each type of reduced- or low-emissions combustor, control strategies can be grouped into general categories. For conventional-appearing combustors, the general categories have been separated into those affecting CO and UHCs and those affecting emissions of NO_x. For unconventional-appearing combustors, the general categories have been separated for convenience by geometric appearance. Regulatory compliance is requiring movement to emissions levels so low that conventional-appearing combustors are unlikely to be satisfactory for the long term.

Control Approaches for Conventional Combustors

Stoichiometry Adjustments for Reduced CO and UHC

Well-stirred reactor (WSR) studies with vaporized or gaseous hydrocarbon/air mixtures demonstrate the following for CO (Ref. 6): For short-residence times and/or low reactant temperatures, CO emissions will be high due to incomplete combustion. For very high temperatures, CO emissions will be high due to dissociation of carbon dioxide. Heavier fuels (high carbon numbers) will have higher CO emissions at given reactor temperature. For short-residence times and low reactor temperatures, UHC emissions will be high due to incomplete combustion. Heavier fuels will have higher UHC emissions at given reactor temperature.

This WSR behavior, which is reaction rate dominated, appears to be paralleled in engines. CO and UHC are predominantly generated at low engine power levels, when significant quantities of both can be evident at idle power settings. Oxidation of CO by the OH radical is an important but relatively slow reaction. It can go to completion if sufficient time is allowed for the conversion, or if the reaction is accelerated. It has been shown⁷ that for earlier engines high-idle power levels of CO in the exhaust were due to insufficient residence time. The design trend toward smaller length combustors⁸ obviates the increased residence time approach. The chemical reaction can be accelerated by raising the concentrations of the reactants, by increasing the temperature of the reactants, and by increasing the reaction pressure, according to the well-known Arrhenius reaction rate expression.

Modern gas turbines tend to idle at higher air pressures and, therefore, also higher air temperatures than did earlier engines. Hence, combustion conditions at low engine powers are slightly more favorable than they used to be. Note, however, that modern engines are unlikely to idle at the 7% power setting that forms a state-point in the ICAO emissions parameters; lower values of 3–5% are more typical. The most dramatic reductions in CO emissions have been achieved by increasing the idle-power bulk equivalence ratio in the primary zone of the combustor, where the flame is held. This is shown in Fig. 1 for an engine operating at idle power.⁹ In Fig. 1, two idle overall fuel/air ratio (OFAR) settings of 0.0126 and 0.0112 are shown, together with variation in the primary zone bulk equivalence ratio. The increase of primary zone bulk equivalence ratio increases the amount of fuel that is burned at and around the stoichiometric value due to fuel/air unmixedness effects.¹⁰ Therefore, the bulk flame temperatures are increased, resulting in the observed improvements in combustion efficiency, which implies reduced CO.

However, it is not immediately clear whether the observed effects in Fig. 1 are truly chemical in origin. Characteristic time studies have been conducted¹¹ for engine primary zones at idle-power conditions, which relate the characteristic time τ ratios for fuel vaporization to CO consumption, fuel/air mixing rates to CO consumption, and

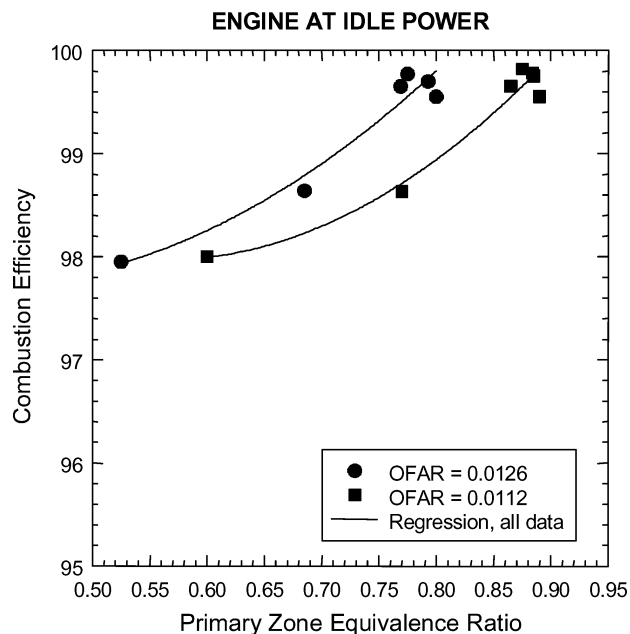


Fig. 1 Effect of primary zone equivalence ratio on combustion efficiency; engine at idle power.

fuel/air mixing rates to fuel evaporation rates. Individual characteristic times may be estimated by the methods of Washam and Mellor.¹² Comparison of the resulting ratios, $\tau_{\text{evap}}/\tau_{\text{CO}} = 1.75$, $\tau_{\text{mix}}/\tau_{\text{CO}} = 3.75$, and $\tau_{\text{mix}}/\tau_{\text{evap}} = 2.14$, shows that CO emissions are physically controlled, in order, by the degree of liquid fuel atomization (because evaporation rate depends on atomization and atomization itself is a very fast process, occurring in typically 10^{-5} s), fuel evaporation, and fuel vapor/air mixing. The behavior shown in Fig. 1 can, therefore, be explained primarily in terms of the increased temperatures resulting in improved evaporation rates of the liquid fuel spray.

The physical nature of CO emissions at low powers suggests that they might be reduced by improving liquid fuel spray evaporation rates through enhanced atomization and by intensifying fuel vapor/air mixing rates. In practice, such steps are difficult to accomplish in a viable fashion. Raising the air pressure drop across the combustor can increase air turbulence; however, high air pressure drop has an adverse impact on engine specific fuel consumption. Atomization from pressure atomizers can be improved by increasing the fuel pressure drop across them at given flow rate, that is, decreasing the injector flow number. However, fuel pump technology has not kept pace with the increased overall pressure ratios (OPRs) of modern engines sufficiently to permit this, even with dual-orifice injectors. Furthermore, the increase in combustor OFARs for improved engine thermal efficiency and higher specific thrust increases the ratio of maximum-to-minimum fuel flow rates (turn-down ratio), which increases the difficulty of pumping hot, low-lubricity fuel. Airblast atomizers can benefit from an increased air pressure drop across the combustor, but again, this adversely impacts engine performance. Atomization and fuel/air mixing can be enhanced by increasing the number of fuel injection points into the combustor. Unfortunately, this increases engine cost and must be done without reducing the individual fuel passage sizes to levels where internal coke formation arising from thermal degradation of the liquid fuel becomes a problem. For these reasons, adjustment of the primary zone bulk equivalence ratio at idle power conditions remains the most powerful tool for control of CO emissions in conventional combustors.

Recirculation Zone Changes for Reduced UHCs

Characteristic time studies relating the rates of CO consumption to hydrocarbon consumption times as a function of primary zone bulk equivalence ratio at idle power conditions show that, chemically, hydrocarbon consumption is tens of times faster than CO

consumption.¹¹ Therefore, for relatively high primary zone equivalence ratios at idle, there should be an insignificant emission of UHCs. WSR studies⁶ support this experimentally. This behavior was not at all the case in earlier engines, where the emission indices (EI) (grams pollutant per kilogram fuel burned) of CO and UHCs were comparable. Again, this suggests some physical control of UHC emissions.

Figure 2 shows the EI of UHC plotted against the EI of CO for several different engines along engine operating lines. The engines are both large and small and are by different manufacturers. Note that the different engines have similar characteristics where, as engine power level is increased from idle [upper right-hand side (RHS) of Fig. 2], the EI of CO and UHC decrease exponentially together at first as the combustion environments increase in pressure and temperature. However, at some point, CO continues to decrease but UHC emissions remain fixed at a plateau level. From a chemical standpoint, this behavior is counterintuitive because CO is derived from reaction of hydrocarbons and CO consumption is much slower than hydrocarbon consumption and, again, supports the idea of some physical control of UHC emissions.

For reasons associated with the recirculation flow patterns contained within the combustor primary zone, liquid fuel injection systems have traditionally been designed to provide a near-90-deg hollow-cone spray angle, as shown in Fig. 3. Liquid fuel droplets can be seen in the flame structures, which are illuminated with a green laser beam.¹³ The upper and lower edges Fig. 3 represent the

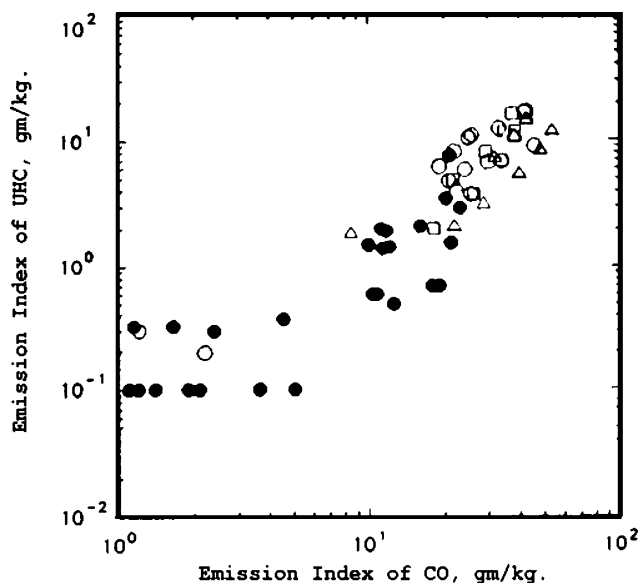


Fig. 2 Relationship between CO and UHC emissions for several engines down an engine operating line.

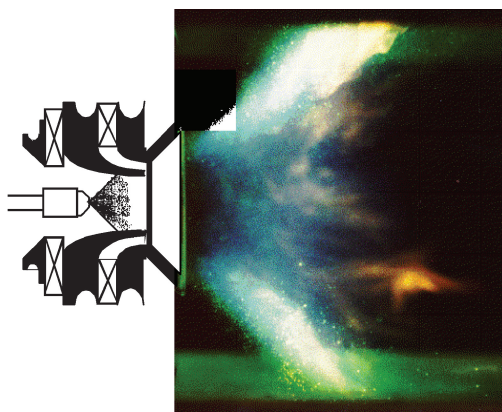


Fig. 3 Laser-illuminated photograph of 90-deg hollow-cone liquid fuel spray in model combustor primary zone.

edges of the optical access in the combustor and not the combustor liners, which are just out of view. However, it can be appreciated that liquid fuel droplets, fuel vapor, and partially reacted fuel vapor in the narrow shear layers of the 90-deg conical spray do reach the combustor liners at the low engine power conditions. On the surfaces of the combustor liners are relatively low-temperature cooling air films to protect the liners from thermal damage. The cooling films entrain and trap the liquid fuel, fuel vapor, and partially reacted fuel vapor. These entrained materials become chemically frozen in the relatively cool cooling air and are progressively diluted with each subsequent addition of cooling air along the liner surface. The chemically frozen constituents exit the combustor along with the cooling air without mixing in again with the hot mainstream. This is primarily the origin of UHC emissions at low engine power levels and is the reason for the behavior seen in Fig. 2.

Elimination of liner film cooling would largely solve the UHC problem at low engine power, and this technique is used in industrial gas turbines for power-generation burning gaseous fuels where high exterior convective air velocities and extended surfaces to enhance heat transfer are used. The combination of operating conditions with a high radiative heat load in aircraft gas turbines is such that reliance on combustor external cooling is not presently viable under most circumstances. Typical combustor liner cooling schemes used to use about 30–35% of the total combustor airflow, W_{AB} . Advanced cooling schemes, such as Pratt and Whitney's FloatwallTM, together with advanced materials, such as cast turbine alloys and single crystals, can reduce the cooling airflow down to 20–25% W_{AB} with excellent durability. Multihole cooling schemes bring manufacturing cost reductions and excellent durability for about 22% W_{AB} . The introduction of new molybdenum-based alloys together with the multihole approach could bring cooling down to 20% W_{AB} or less. Thermal barrier coatings (TBCs) can be used to advantage with all of these schemes. TBCs in aged condition, are worth about 100°F in liner temperature. Although these represent very useful reductions in cooling air, they are not sufficient of themselves to significantly reduce UHCs.

The root cause of the difficulty, which is one of fuel entrainment into the dome and liner cooling air films, is associated with the conventional recirculation zone traditionally used for flame stabilization in the primary zone.¹⁴ As can be seen from Figs. 3 and 4a, when used with a 90-deg spray angle fuel injector, this flow pattern directs raw fuel straight into the combustor liner wall region. These difficulties can be addressed by turning the conventional recirculation zone inside out in the manner of Fig. 4b.

The flow patterns of the inside-out recirculation were based on visualizations made in a water analogy rig. The inside-out recirculation can be achieved through a combination of two means: first, using an airblast atomizer fuel injector of modest air-swirl angle and with air passages that converge on the injector tip centerline and second, using a combustor dome within which the two-phase discharge from the fuel injectors experiences an immediate and significant sudden expansion on entering the combustor. The swirling discharge from the injectors maintains its coherence for a significant distance into the combustor. Eventually, the combination of swirl and entrainment demands cause large exterior recirculations to develop around and between individual injector discharges. Small recirculations internal to the swirling jet flow are developed under the combined influences of vortex bursting and the backpressure effects of the penetrating transverse combustion air jets from the liners. The position of the combustion air ports is a little farther downstream than is usual to facilitate the initial coherence of the fuel/air jet from the injector. As shown in Fig. 4b, there is a flow conflict between the large outer recirculation zones developed around the swirling jet and the dome and primary zone liner film cooling air. To optimize the flow patterns, the cooling air films in the dome and primary zone could be reversed in direction¹⁵ so that shear is reduced and recirculation strengthened.

Figure 5a shows the flame structure for an inside-out recirculation at lower power levels (injector equivalence ratios less than unity) by natural light, in the same model combustor as in Fig. 3. It can be seen that the flame is confined to the central region of the

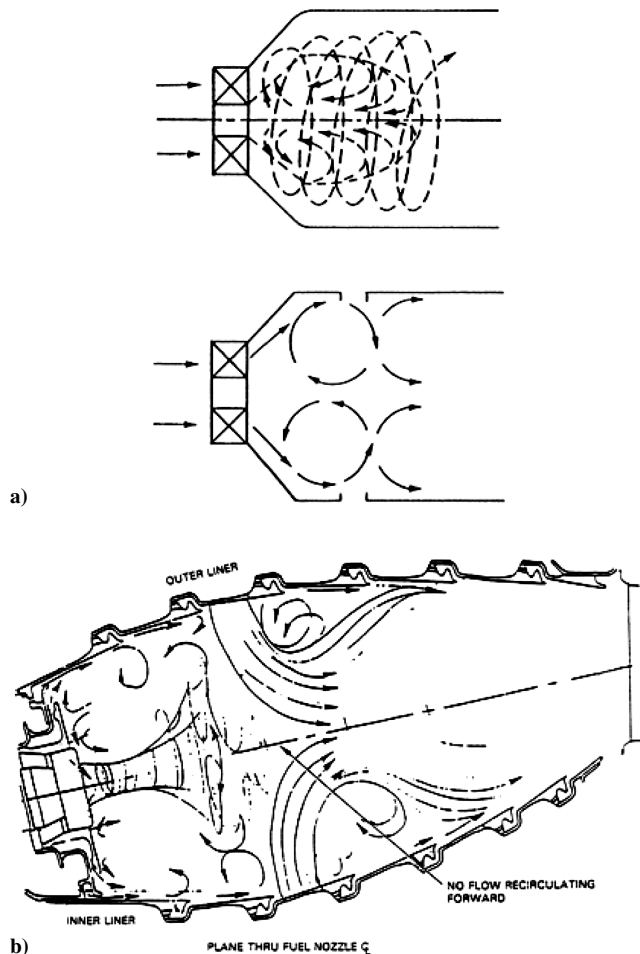


Fig. 4 Comparison of recirculation zones: a) conventional and b) inside out.

combustor. Flame holding is provided by means of a very small central recirculation zone [not visible here but shown by laser Doppler velocimetry (LDV) measurements] and large corner recirculation zones formed between the combustor dome, the liners, and the central flames and between the dome and adjacent fuel injectors.^{16,17} Composite planar laser-induced fluorescence (PLIF) images of OH (Fig. 5b) indicate regions of heat release and show that very little reaction takes place in flow that is recirculated to the liners and back into the dome for injector equivalence ratios that are less than unity, which is typical of idle power values. Separate laser doppler velocimetry LDV and coherent anti-stokes Raman spectroscopy (CARS) measurements revealed the recirculation patterns, which were similar to those shown in Fig. 4b.

The UHC engine emissions for a combustor having an inside-out recirculation zone and an advanced cooling scheme are compared in Fig. 6 with those for an engine having a conventional combustor design. The engine power level is represented by means of the compressor exit air temperatures, which essentially correspond to the temperature of the cooling air introduced onto the liner surfaces. It can be seen that, for the same operating conditions, the inside-out recirculation zone in the primary zone yields significantly lower UHCs. It can be shown that the major contribution of the UHC reduction is due to the recirculation zone changes.

A reasonable concern for the inside-out recirculation zone is that the concentration of fuel in the coherent swirling jet and the initial region of the bursting vortex might result in the generation of large amounts of CO from locally overrich mixtures. This possible tendency would be exacerbated by the selection of a relatively high (but less than unity) primary zone equivalence ratio at idle to speed liquid fuel droplet evaporation rates through high flame temperatures. Experience shows that this is not the case due to burn-up of CO in the intermediate zone of the combustor. CO levels were about half

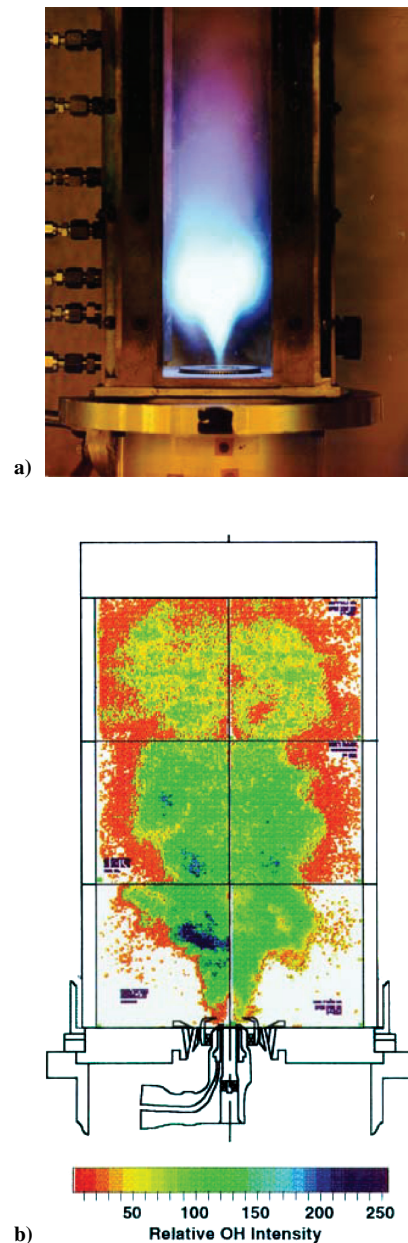


Fig. 5 Inside-out recirculation zone: a) natural light flame photograph and b) PLIF OH image.

those for a conventional recirculation zone. Of course, it is essential to ensure that the design of the intermediate zone is suitable to achieve the necessary CO burn-up. This involves appropriate selection of intermediate zone bulk temperature, mean residence time, and intermediate air jet patterns. For example, a suitable intermediate zone length of one-half a dome height and a mean equivalence ratio on 0.6 might represent appropriate values.

Similarly, the potential for locally overrich fuel/air mixtures due to the inside-out recirculation pattern, together with the use of high primary zone equivalence ratios at idle power, suggests a propensity for excess smoke generation at high-power levels. This is a genuine concern that is addressed by the introduction of very small quantities of smoke control air in close proximity to the fuel sources. However, UHC emissions may then rise at low power if significant quantities of relatively cool compressor air are introduced directly into the flame region. The chilling effects of such air can exert a powerful influence on local reaction rates that is reflected in a sharp increase in UHC emissions. This is shown in Fig. 7, which shows the UHC emissions at idle power for an inside-out recirculation zone as a function of the sum of injector and smoke control air. The UHC curve is essentially the reciprocal of the high-power smoke curve

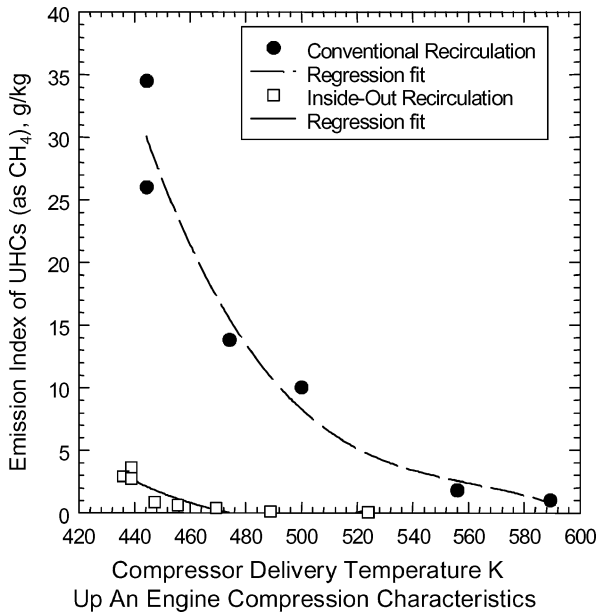


Fig. 6 Comparison of UHC emissions for conventional and inside-out recirculation zones.

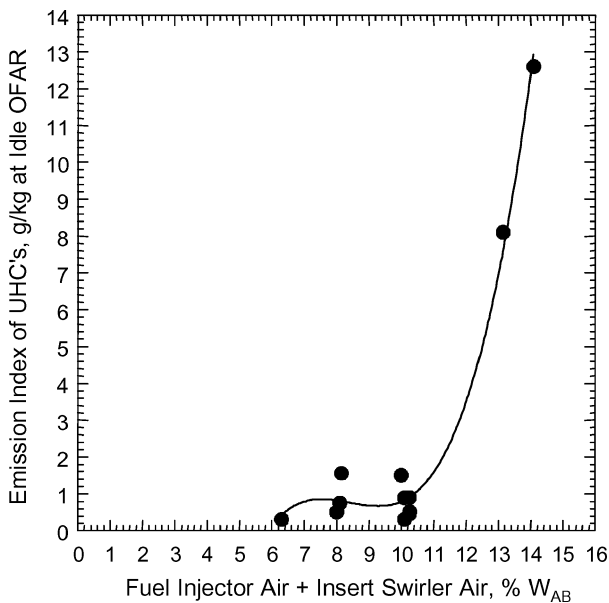


Fig. 7 Effect on UHC emissions of air injection into flame at idle power; PW experimental JT9D-70A engine.

for this engine. It arises because excess air introduced in this fashion results in a dome equivalence ratio that is too low; minimum UHC emissions were achieved when the dome equivalence ratio was unity. The UHC emission was relatively insensitive to the direction of the swirl of the smoke control air. With this type of arrangement, peak exhaust smoke is attained before maximum power. This is due to smoke particle burn-up immediately downstream of the inside-out recirculation zone when sufficiently high gas temperatures are reached.

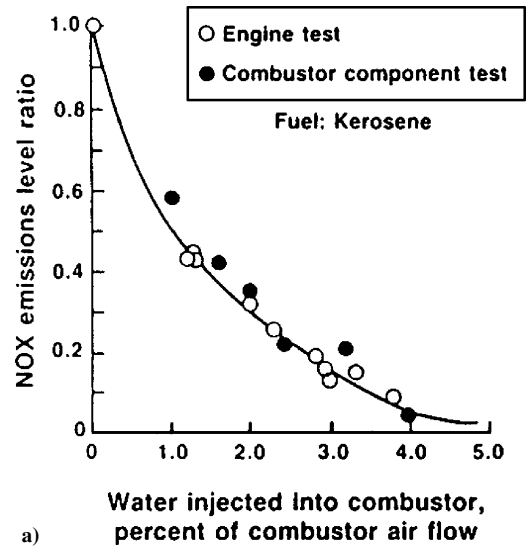
By the means described, a favorable balance between low-power emission of CO and UHC and high-power smoke can be obtained. This forms an example of the interemission trading that was referred to earlier. The strategy proved portable engine-to-engine and was even more effective when used in conjunction with advanced liner cooling schemes.

Adjustments of Time/Temperature History for Reduced NO_x

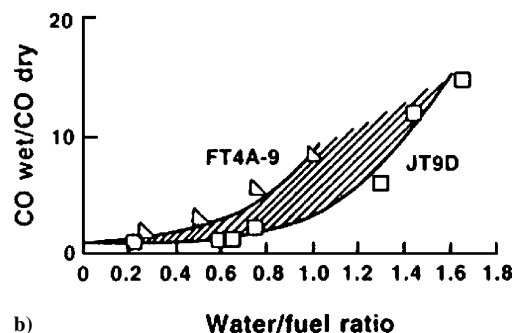
Large amounts of NO_x are produced at high engine power levels, and at the engine exhaust, the NO_x consists mainly of nitric oxide, NO. Characteristic time studies¹¹ at engine conditions relating NO generation of hydrocarbon consumption illustrate clearly that NO is a postflame phenomenon for all ranges of likely equivalence ratio. These studies also show that NO generation is a slightly faster chemical process than is CO consumption, and hence, trade-offs between NO and CO will exist. WSR experiments⁶ confirm that NO emissions will be high for long-residence times and/or high reactor temperatures. Thermal NO, produced by the extended Zeldovich-Lavoie mechanism, which represents oxidation of atmospheric nitrogen, is a postflame phenomenon that is time-at-temperature driven. Therefore, early attempts at NO_x control aimed to cut both time and temperature by any means available.

Simply shortening the combustor can reduce the residence time. However, significant reductions in NO_x require significant reductions in residence time. Typically, a 60% reduction in primary zone residence time only results in about a 40% reduction in NO_x (Ref. 11). Unfortunately, at the greatest reductions in residence time, the combustion efficiency has also fallen dramatically to levels considerably less than 90%, and flame stability is seriously impaired.

NO is only sparingly soluble in water. Water, however, has a significant latent heat of vaporization and, therefore, offers an effective means of reducing flame temperatures, especially if it is introduced close to the fuel source.¹⁴ Injection of water equal to about 3% W_{AB} will reduce NO_x by 80% (Ref. 11). Figure 8 shows the NO_x reduction where the water is expressed in terms of the combustor airflow, and it can be seen that worthwhile NO_x reduction requires a water flow that is comparable to the fuel flow, as well as that CO emissions can be increased. However, this represents a considerable quantity of



a)



b)

Fig. 8 Water injection into conventional combustor primary zones: a) NO_x reduction and b) CO increases.

water so that the technique would only be used on takeoff and initial climb-out. Therefore, there would be no NO_x control at altitude due to water injection. The water quality would have to be boiler-feed standard to avoid scale fouling of the turbine cooling system. The mass addition of the water can provide worthwhile engine thrust augmentation, which can be helpful for hot day, high-altitude take-offs. After the water has been injected the water tanks, distribution pipes and controls represent an increase in aircraft deadweight.

Quasi-Staged Rich–Quench–Lean Combustion for Reduced NO_x

Use of an elevated combustor primary zone equivalence ratio in the range of 0.8–0.9 at engine idle to minimize low-power CO emissions allows advantage to be taken of the reduced flame temperatures at high power that result from over-stoichiometric combustion. This over-stoichiometric primary zone behavior arises because of the fixed geometry of the conventional combustor,¹⁸ where there is a linear relationship between primary zone equivalence ratio and OFAR. A primary zone equivalence ratio set to around 0.8 at idle results in a value between 1.5 and 2.0 at takeoff with typical turndown ratios. Rich burning at takeoff suppresses the peak NO_x emissions attained. The efficacy of the approach is limited by fuel/air unmixedness effects, by the existence of stoichiometric interfaces, and by the onset of excess exhaust smoke. The first of these limitations is demonstrated in Fig. 9.⁷ Mixing studies¹⁰ indicate that there is little benefit of operating with initial burning zone (IBZ) equivalence ratios in excess of about 1.4.

The process was originally thought of simply as another time vs temperature control technique. However, general acceptance of the Fenimore prompt-NO process¹⁹ modified the view of the concept. Combustion at high temperatures in an oxygen-deficient atmosphere results in atmospheric nitrogen reacting preferentially with hydrocarbon fragments produced by fuel-cracking reactions. Subsequent reaction of these modified fragments that now contain chemically bound nitrogen, very efficiently and rapidly produces NO. This secondary reaction usually takes place in a fuel-lean atmosphere. For this reason the process is labeled as rich–quench–lean (RQL) burning and is given a separate category.

With fuel-rich burning in the primary zone, unburned fuel (as lower hydrocarbons containing bound nitrogen, soot, and CO) will enter the intermediate zone [or secondary burning zone (SBZ)] of the combustor, even with 100% oxygen consumption efficiency in the IBZ. The duty of the SBZ, therefore, undergoes a shift in emphasis. Its primary role shifts from CO burn-up at low powers and high-altitude cruise conditions²⁰ to CO, UHC, and soot consumption at high power. To complete this combustion process, the SBZ will operate fuel lean. To accomplish its expanded function, the combustion air jet array feeding the SBZ has to provide adequate

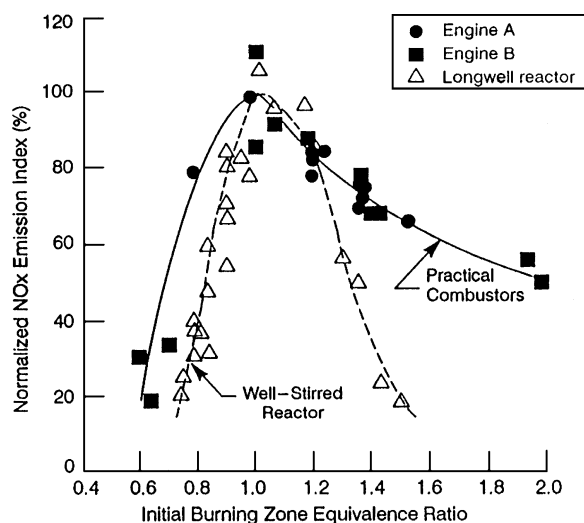


Fig. 9 Effects of primary zone (or IBZ) equivalence ratio on normalized NO_x emissions.

flame holding capability to confer satisfactory static stability on the combustor. The transverse air jet array then becomes the major source of NO_x generation due to the burn-up of the fuel fragments with their bound nitrogen, which produces in-flame NO and, subsequently, postflame NO through the Zeldovich–Lavoie mechanism. This is shown in Fig. 10 for a model combustor,²¹ where the pairs of air jets of equal and various diameters are opposed to each other and are positioned with a pair of jets placed inline with the fuel injector. Burning takes place around the jets and over the recirculation zone formed by their convergence, on the centerline of the combustor.

Design maps for this RQL approach as implemented in a conventional combustor geometry can be produced⁷ that link relative NO_x and IBZ and SBZ equivalence ratios. As an example, from such a map an engine operating with an IBZ equivalence ratio of 1.5 would have 50% of the NO_x of a conventional combustor of the same residence time if the SBZ had an equivalence ratio of 0.35. Figure 11 shows the measured NO_x reduction achieved in an engine with this simple type of RQL compared to the conventional combustor for the engine; engine power level is represented by combustor OFAR.

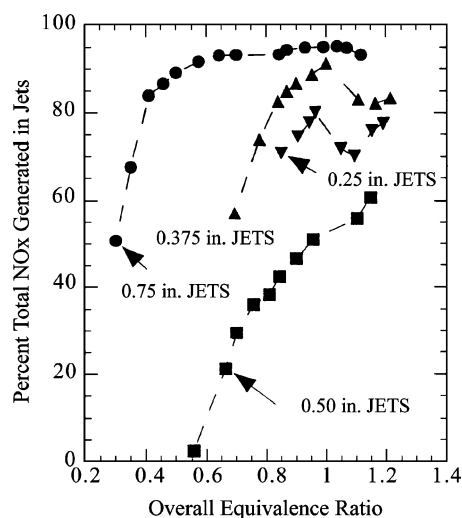


Fig. 10 Demonstration in model combustor of jet contribution to NO_x for lean SBZ with rich IBZ.

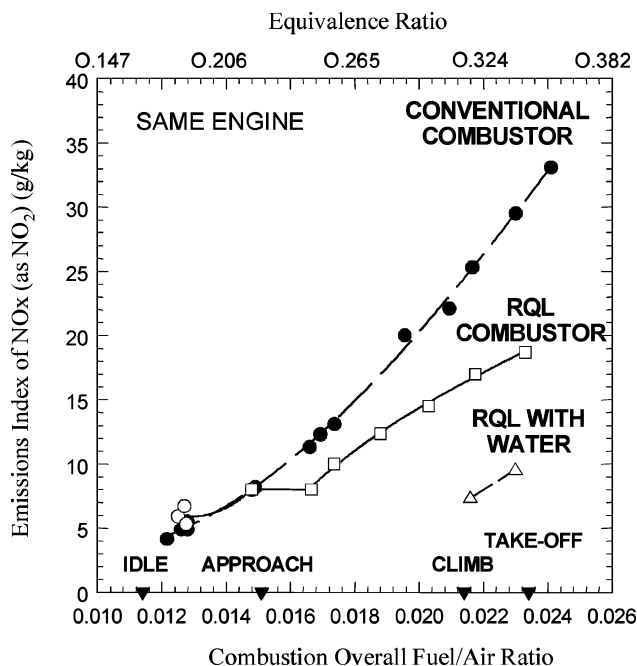


Fig. 11 Engine measured NO_x reductions with simple ROL combustor and with water injection.

It can be seen that with the RQL, NO_x at idle is increased slightly, and this reflects the elevated equivalence ratio for enhanced combustion efficiency. Noteworthy is the clear hesitation in NO_x around the approach power level, where NO_x remains fixed although engine power is increased. This hesitation is due to the IBZ reaching and then just exceeding unity equivalence ratio, where unmixedness suppresses NO_x and where the unburned fuel quantities entering the SBZ are low, giving very low equivalence ratios and, hence, a negligible SBZ NO_x contribution. This hesitation is in some respects similar to fuel staging, hence the use of the term quasi staging in the heading. It represents a form of axial staging and was dubbed quasi staging to distinguish it from mechanical axial staging, which is to be discussed later. At higher power levels, more and more unburned fuel leaves the increasingly richer IBZ. Mean equivalence ratios in the IBZ, therefore, increase, and IBZ NO_x starts to dominate total NO_x production. Further increases in power setting give an increase in NO_x. However, note that the NO_x curve for the conventional combustor is slightly but definitely concave upward whereas that for the RQL combustor is slightly but definitely concave downward. This behavior of the two curves results in a favorable divergence in NO_x for the RQL combustor as the engine power increases. This characteristic is due to fuel/air unmixedness effects in the IBZ as its equivalence ratio increases. Eventually, however, at higher power levels than those shown, the IBZ would in turn become stoichiometric, resulting in another NO_x hesitation until NO_x due to burning in the combustor dilution zone becomes dominant. Therefore, if smoke controllability limits the maximum IBZ equivalence ratio that can be used, then the RQL control approach is apparently limited in maximum OFAR capability.

As a matter of interest, this RQL realization was also evaluated with water injection (Fig. 11). The combination achieves a NO_x reduction at takeoff power (to the same OFAR) of 60%. The water in this instance was introduced in an expedient fashion and was not optimized in any way. NO_x along an operating line with water injection would follow the RQL curve until climb. At climb, water injection is turned on and NO_x drops instantaneously to the water curve, which is then followed through takeoff power.

Control Approaches for Unconventional Combustors

Optimized RQL

There are two major difficulties with the RQL as described for conventional combustors. These are 1) the necessary provision of liner cooling resulting in the formation of stoichiometric interfaces in the IBZ and 2) slow mixing rates resulting in the formation of stoichiometric interfaces around the transverse air jets in the SBZ. These two sets of stoichiometric interfaces are responsible for the generation of excess NO_x. Addressing these issues results in a combustor that is unconventional in appearance.

As part of NASA's now canceled high-speed civil transport (HSCT) program, Pratt and Whitney produced an optimized RQL combustor design²² that was functionally similar to that described earlier and embodied two burning zones in series while addressing the issues efficiently. The fuel-rich IBZ of the design was externally cooled via a closely fitting shroud to provide high convective cooling velocities. The convective cooling air for the IBZ, having completed its cooling task, then formed the quench air jets necessary to lower the bulk equivalence ratio to fuel lean for the SBZ. The quench air jets were introduced in a reduced cross-sectional area mixing section that was additional to the nonoptimized RQL configuration. The reduced flow area, together with the mass addition of the quench air, accelerated the internal gas flow to high velocities in an attempt to prevent burning from taking place in the mixing section. The SBZ was a short dump combustor immediately following the mixing section.

Several complications were encountered during development of this combustor. The best overall mixing for a quench section is provided with an optimum jet momentum flux for opposed jets that precludes direct jet impact. Therefore, it was extremely difficult to avoid a situation where, before mixing was complete, stoichiometric flames formed around the entering quench air jets. The high temperature of the spent cooling air forming the quench jets exacerbated this tendency.

In an attempt to address this issue, Pratt and Whitney introduced a can-annular configuration, where the IBZ was made up of 12 individual circular cross section cans, each with its own fuel injector, external cooling, and quench air jet system; the SBZ was annular. A later configuration was fully annular because these problems were eventually solved by working on the quench air patterns, although details of this have not been released. It also proved necessary to use nonmetallic ceramic composite liners for the IBZ. Finally, due to the high OFAR turndown ratio necessary for supersonic operation of the engine, the design ran into IBZ/SBZ equivalence ratio and smoke problems, as mentioned earlier. These were solved through use of variable-geometry fuel injectors that provided a limited degree of IBZ air modulation. The resulting combustor pressure loss changes were uncompensated without serious performance penalties.

Pratt and Whitney conducted parametric measurements of the emissions for this combustor in rigs and determined the pressure sensitivity of NO_x. With use of these scaling laws applied to the engine of Fig. 11 (without water injection), this optimized RQL design technology could have a takeoff NO_x falling slightly lower than halfway between the quasi-staged RQL dry and the quasi-staged RQL with water injection. This would represent an NO_x EI of about 12 g/kg. This signifies a creditable performance, that is, a 65% reduction in takeoff NO_x compared to the conventional combustor.

Staged Combustors

The consequences and limitations of a fixed-geometry combustion system have been mentioned already. If some form of staging is introduced, the combustor characteristic governing zone and overall equivalence ratios can be made much more flexible.¹⁸ Aeroderivative gas turbines for industrial power generation have been successfully produced (after great effort), with multiple-stage combustors.²³ However, whereas staging appears relatively simple, control of staging in an engine with a wide range of operating conditions is very complex. Part of the control complexity is that staging must not occur at any engine steady-state operating points to avoid hunting. Any staging system must also have a fast response in emergency conditions, and so a design requirement is that the combustor must always be fully staged when in the vicinity of critical flight conditions. Staging of course, must be completely transparent to the pilot. By this is meant that there should be no thrust bumps during the process. In addition, the pressure pulse propagated upstream as the main stage ignites must not adversely affect the engine compression system. Furthermore, there is the issue of liquid fuel coking in fuel injector passages due to heat soakback in stages that are shut down while the engine is operating at some power level. For these reasons, only two-stage combustors have been considered so far for aircraft applications. Either the airflow (as in the Pratt and Whitney optimized RQL combustor for the HSCT) or the fuel flow can be the quantity that is modulated. Generally, there are serious difficulties associated with air modulation, and so staging is usually applied to the fuel supply only.

Fuel staging normally implies that the combustor possess two separate burning zones, each fueled separately. The separate burning zones are commonly referred to as the pilot stage and the main stage. Functionally, the pilot stage fulfills most of the duties of a primary zone, whereas the main stage fulfills many of the duties of the intermediate zone of a conventional combustor. Engine starting and idling is accomplished on the pilot stage. At some point before an approach power condition is reached, the main stage is fueled and ignited. For all power levels above approach, both stages will be operated; however, the fuel split between stages can be adjusted by the fuel controller if so desired, to suit operating conditions and to minimize emissions.

The two burning zones can be arranged in one of three fundamental configurations: axially, radially, or circumferentially. The circumferential arrangement is extremely convenient because the combustor only differs from a conventional design in its fuel system. However, the circumferential arrangement is not favored because of the asymmetric temperature distribution for pilot-only operation

that can cause out-of-roundness problems for the turbine casings. Also, the chilling effects of the cold airflows at the edges of the unlit main stage bordering the operating pilot stage can result in an increase in low-power CO and UHCs. Figure 12 shows an example of a radially staged combustor by General Electric (GE). The main stage is placed inboard of the pilot stage, and the stage fuel injector tips are placed on a common support stem. The configuration results in a short and deep combustor that requires a complicated prediffuser design. The combustor, thus, has two separate flames arranged in parallel when both stages are fueled, and these flames are in communication with one another. Two separate flames that are in communication can “talk” to each other, and acoustic coupling can occur. This is a possible difficulty with the radial arrangement.

Axial staging, where a conventional upstream pilot feeds hot gases into the downstream main stage thereby assisting main stage lightoff and subsequent burning, does not necessarily result in an increase in combustion section length. Pratt and Whitney (PW) engine demonstrated an axially staged combustor (ASC)²⁴ that had 20 airblast-atomizing fuel injectors in each stage and had the same overall burning length of the quasi-staged RQL combustor it replaced. The pilot stage used inside-out recirculation technology. A similar combustor has been explored by Rolls-Royce Deutschland,^{25,26} where

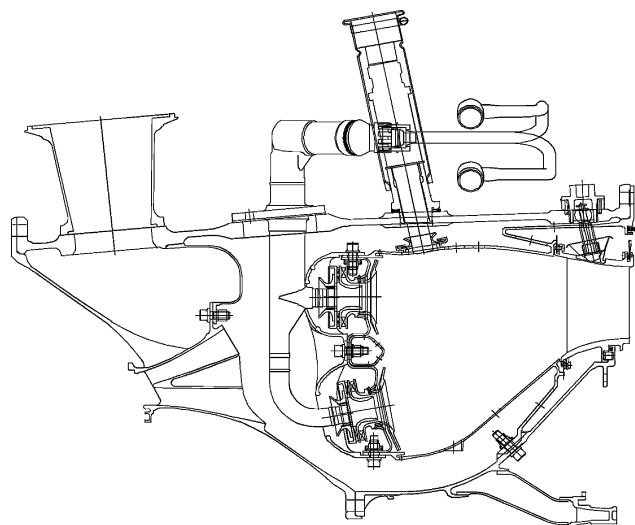


Fig. 12 Staged combustion, GE radially staged combustor (International Symposium on Air Breathing Engines) (ISABE Paper 2003-2657).³¹

it was found that careful optimization of the interactions between the two stages is necessary to achieve the best emissions. The PW ASC had an optimized pilot stage, where at engine idle the NOx was acceptably low (around 5 g/kg) while maintaining good stage efficiency (greater than 99.9%) and lean blowout (LBO) overall fuel air ratio (OFAR) capability 40% or more below the most severe requirement. The integrated emissions values for the demonstrator engine were 46.6, 35, and 1.75% of the 1996 ICAO regulations for NOx, CO, and UHCs, respectively, although note that the values for CO and UHCs were actually increased over those for the baseline engine. However, the baseline engine had very low values of CO and UHC emissions so that this was not a concern. Again, this is an example of emissions trading. Figure 13 shows a cross section of the ASC, where the main-stage fuel injectors for convenience are shown in the same plane as the pilot-stage injectors; actually, they were staggered relative to the pilot-stage injectors. The ASC was accommodated in the same pressure casings as the baseline combustor, with the only necessary modifications being the addition of pads to the outer casing to accept the main-stage fuel injectors. There was only a single ignitor plane (in the pilot stage).

The behavior of staged combustion is important and is best understood by considering the individual emissions characteristic variation with engine power.²⁷ The engine power level is here represented in terms of combustor inlet temperature, and Fig. 14 shows the CO, NOx, and UHC characteristics, respectively, for the ASC. The staging point is clearly identifiable by fairly massive increases in CO and UHC emissions and by a modest decrease in NOx. The NOx characteristic should be compared to that shown in Fig. 11 for the quasi-staged combustor. The shift in the NOx curve is ultimately the same, although it is achieved differently. Although the main stage of the ASC is assisted by the entering hot effluent from the pilot stage, initial combustion in the main stage when it is fueled is not easy, and the subsequent recovery of low CO and UHC emissions is slow. At the staging point, the overall combustion efficiency can be as low as about 90%. This behavior is typical for fuel-staged systems whatever their arrangement. In some instances, the loss in efficiency and slow recovery have been severe enough to result in unacceptable fuel-burn problems for the engine. The reason is the very lean main stage that results as the main fuel comes on immediately following staging. However, this problem can be worked on by means of fuel scheduling and optimized pilot/main-stage interaction. Care has to be taken however, not to introduce thrust bumps.

Staged combustors have been accepted as low-emissions combustors because staging takes place well away from any operating condition used for compliance evaluation. How they actually work as emissions control devices can best be illustrated by comparing

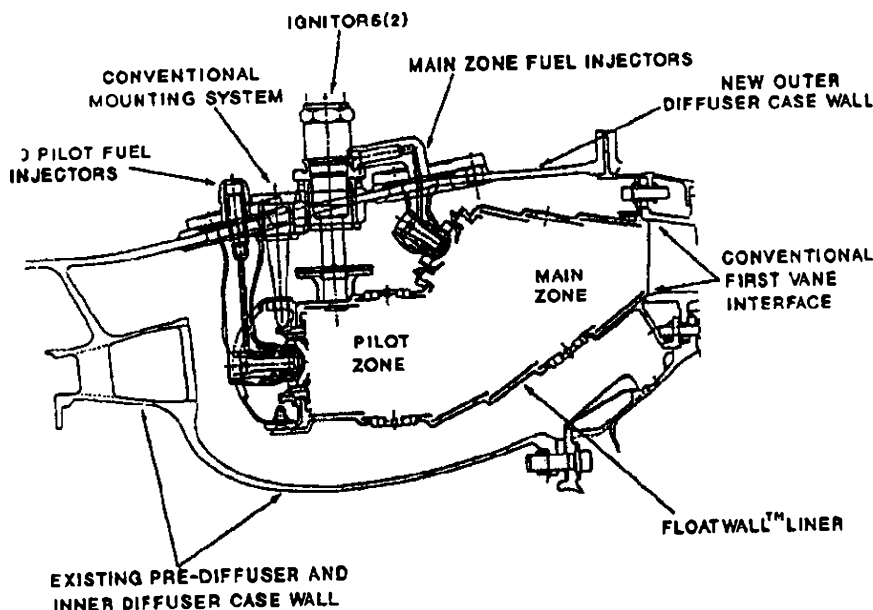
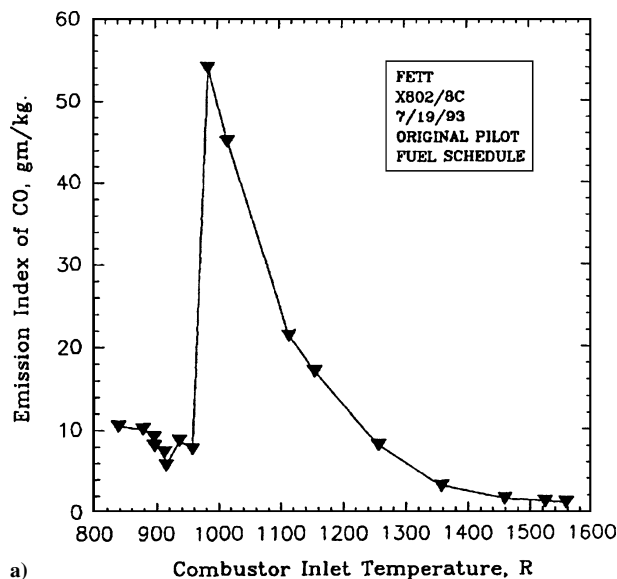
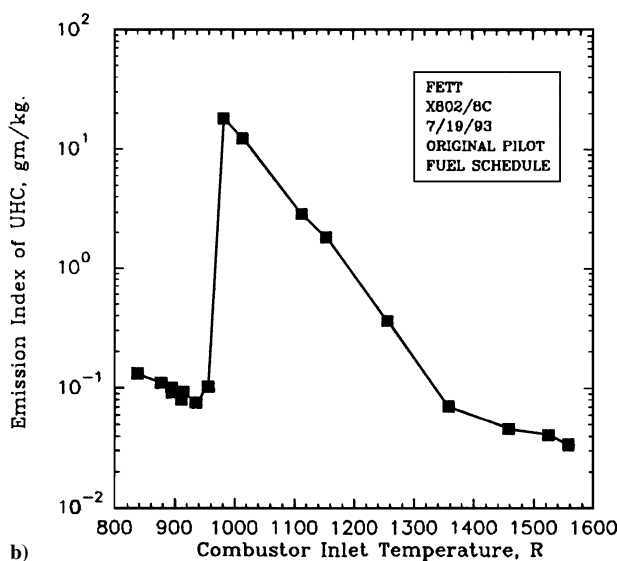


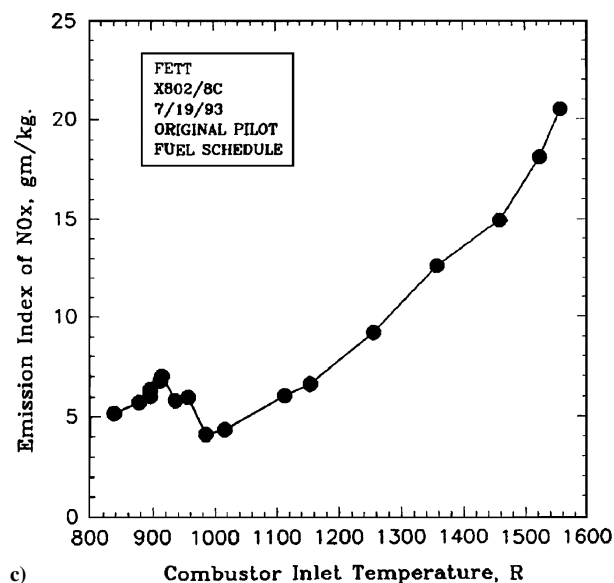
Fig. 13 PW's ASC as tested in IAE V2500 engine.



a)



b)



c)

Fig. 14 Effect of power level on emissions indices for staged combustor (PW ASC, first engine to test).

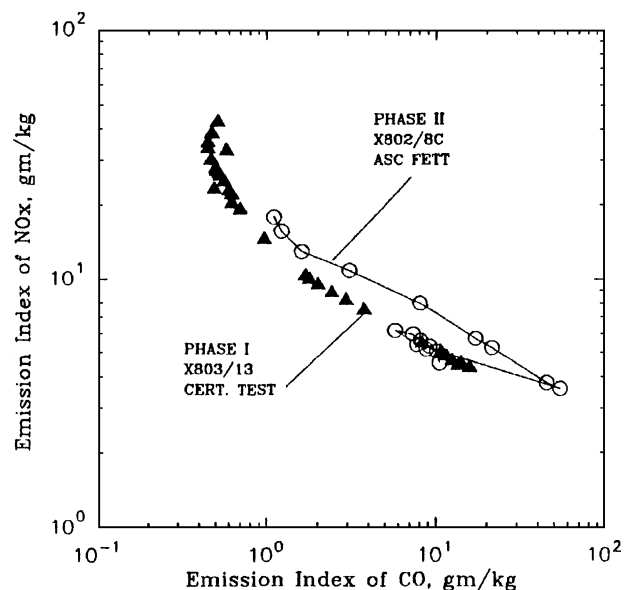


Fig. 15 Comparison of emissions tradeoffs for ASC and quasi-staged RQL combustors.

NO_x vs CO for the ASC and quasi-staged RQL combustors, in Fig. 14.

For a CO vs NO_x trade as shown in Fig. 15, movements of the curve toward the origin represent true overall emissions reductions, and movements along a curve represent a tradeoff between CO and NO_x. In Fig. 15, the solid triangles represent the quasi-staged RQL combustor and the open circles represent the ASC combustor that replaced it; the engine model is the same in each case, and the engine numbers and builds are given. For the quasi-staged RQL combustor, the idle point is at the lower RHS of Fig. 15, and as engine power is increased, the plot is followed smoothly up the operating characteristic to the upper end of the curve, which represents takeoff power. For pilot-only operation, the ASC data points at the lower RHS follow identically those of the quasi-staged RQL combustor, which is as it should be because both use the inside-out recirculation and associated technology and have identical numbers of fuel injectors. When the ASC is staged, however, the curve is folded back on itself and moves far to the lower right of Fig. 15, which represents the maximum CO and minimum NO_x condition; see Fig. 14 also. As power is further increased with both stages operating, the CO slowly is reduced and the NO_x increases. The after-staging portion of the ASC curve is displaced to the right of the quasi-staged RQL curve. Because the ASC curve is to the right of the quasi-staged RQL curve, the ASC clearly represents an inferior overall low-emissions technology. It does so well in terms of the integrated emissions parameters because 1) the emissions are low at the very limited number of set points for which the ICAO integration is performed and 2) because the inside-out recirculation technology is so good that it permitted some NO_x vs CO trading to be made. The ASC is, therefore, an example of trading emissions to advantage.

Improved Mixing, Lean-Burn Staged Combustors

For staged combustors, the pilot-stage contribution to the total NO_x can be dominant unless the pilot fuel is modulated at high-power levels. When this is done, the pilot contribution to total NO_x can become almost negligible. Regardless of the pilot equivalence ratio, the main-stage NO_x for the ASC appears to be virtually independent of the main-stage equivalence ratio.²⁴ These points are shown in Fig. 16, which suggests, with reference to Fig. 9, that the main stage, which processes most of the fuel, is very poorly mixed. This is not unexpected because nothing serious has been done to address fuel/air mixing in these realizations.

Appreciation of the preceding points, together with the recognition of the infeasibility of premixing for aircraft applications, has led to some consideration of and a degree of concentration on, piloted

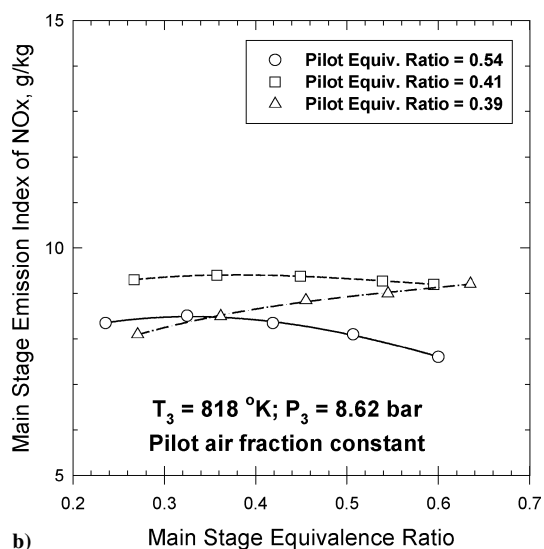
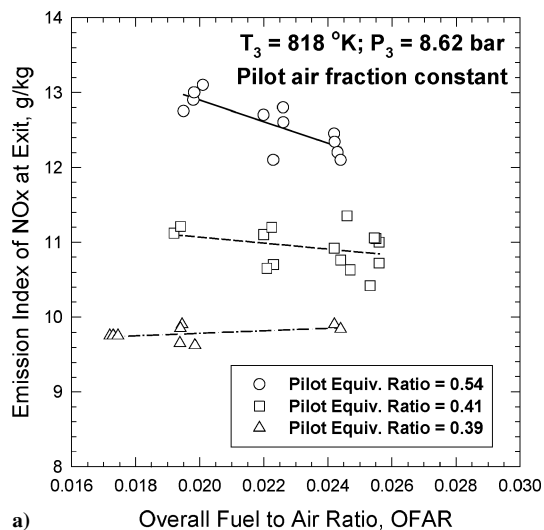


Fig. 16 Contributions to NOx in staged combustor: a) pilot stage and b) main stage.

lean direct injection (LDI) for advanced low-emissions concepts. A pilot of some form is still needed to satisfy engine operability requirements, but serious attempts are made for most of the fuel injected to improve fuel/air mixing such that combustion actually takes place close to the bulk equivalence ratio of the main stage.

LDI concepts can range from those having the pilot stage separated from the main stage (as in radial or axial staging as described earlier) with separate sets of fuel injectors, to those having the pilot stage central to a surrounding main stage in an integrated fuel injector. The pilot stage design can follow the design practices already described including fuel modulation at high power, whereas the essence of the LDI main stage is to improve the presentation of the stage fuel flow to the stage airflow to enhance mixing dramatically. This is accomplished by injecting the stage fuel (which makes up the majority of the total fuel flow) through a large number of atomizer tips. The intent is to approximate the probability distribution function for local equivalence ratio in the main stage to a delta function, that is, to a single-stage equivalence ratio, that is lean. Some designs incorporate main-stage swirl cups intended to allow some fuel spray evaporation and mixing of the resulting vapor with air before combustion. However, constraints of autoignition severely limit this potential. For those concepts that have a central pilot with a surrounding LDI main stage, the resulting flame zones cannot be allowed to merge because experience indicates that low NOx cannot then be achieved. Unfortunately, if the two flame zones, one within

the other, are distinctly separated, they will have a tendency to talk to each other, and acoustic coupling can occur.

How well mixed does the main-stage fuel and air need to be and at what equivalence ratio? Consideration of Fig. 9 suggests that the answers to these questions are respectively very well and quite low. There are many ways in which mixing can be represented but a mixing parameter S (Ref. 28) can be defined as

$$S = \sigma / \tilde{\varphi}$$

where σ is the standard deviation for a Gaussian distribution of equivalence ratio about the mean of $\tilde{\varphi}$ such that $S = 0$ represents perfect mixing. Figure 17 shows the influence of S on the formation rate of NO as a function of mean equivalence ratio. It can be seen that for enhanced mixing to be advantageous, $\tilde{\varphi}$ has to be less than 0.7 and S has to be less than 0.25 for lean combustion. Figure 18 gives estimates for S in practical combustors.¹⁰ Figure 19 shows the implications of Fig. 18 for a conventional pressure drop airblast injector fuel source combustor with a nominal lean-burn primary zone with mean equivalence ratio of 0.6. One, two, and three sigma bands

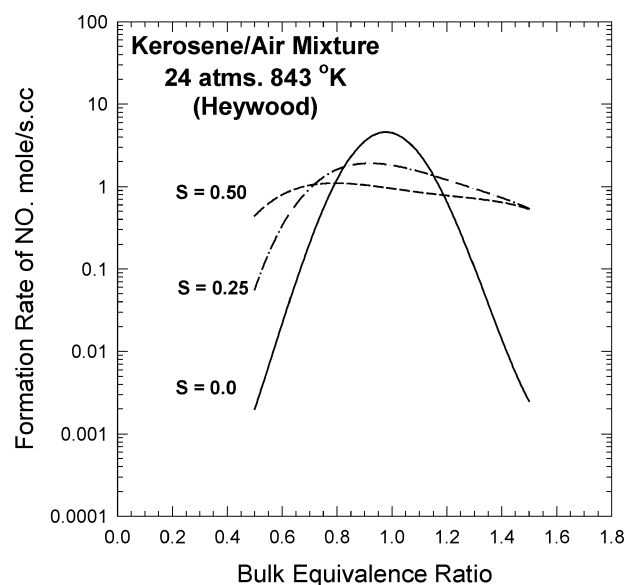


Fig. 17 Effect of mixing parameter on rate of formation of nitric oxide (Heywood and Mikus²⁸).

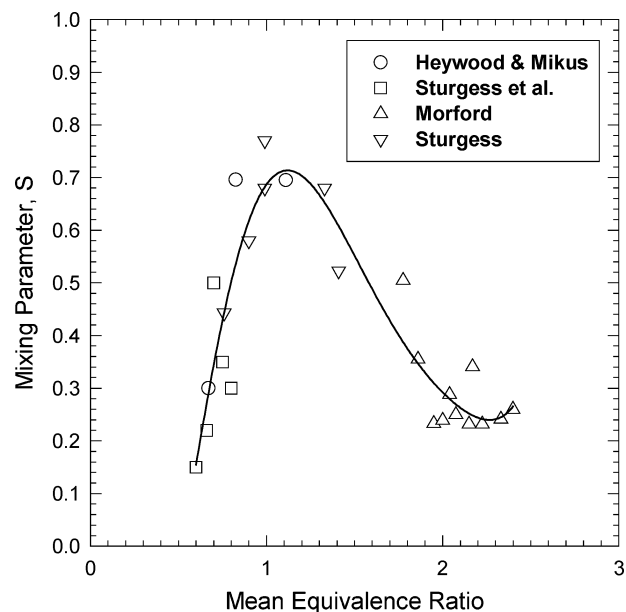


Fig. 18 Collected S experience for variety of practical combustors.

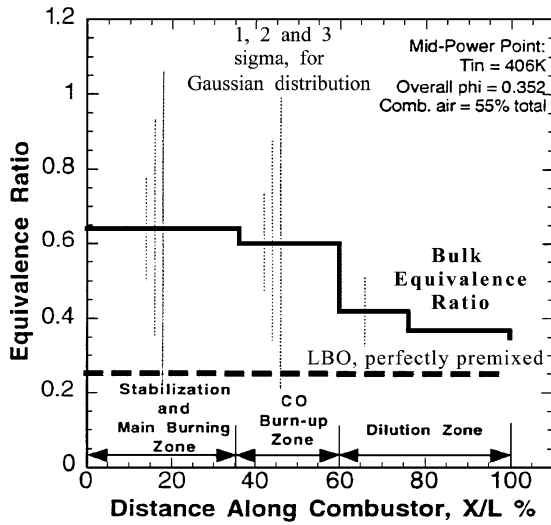


Fig. 19 Implications of fuel/air mixing in conventional lean-burn combustor.

of equivalence ratio for the Gaussian distribution are shown.^{10,11} It can be seen that the fuel really burns over a wide range of equivalence ratios and that some fuel components will actually leave the primary and intermediate zones of the combustor unburned.

For $\phi < 0.6$, Figs. 17 and 18 indicates an S value equal to about 0.10 would be necessary to yield formation rates $d[\text{NO}]/dt$ that are low. To then achieve low NOx emission indices, the mean residence time of products in the hot reaction zone has to be low also. These requirements together establish the design criteria for the LDI main stage.

The mixing parameter S will have two components, one that is associated with the total energy available for mixing in the combustor and one that is associated with the way the fuel is introduced. The total energy is mostly the air pressure drop across the combustor and generally cannot be increased because of the adverse effects on engine specific fuel consumption; the fuel introduction component includes the atomization level provided and the way the fuel sprays are presented to the air. It is mainly this latter component that LDI combustors seek to address by making large increases in the number of fuel sites. The main stage of the ASC, for example, had 20 injectors, whereas the main stage of an LDI combustor might have 100–200 fuel sources at a minimum. Typically, there might be 20 injector supports, each carrying 5–10 spray tips. One extreme example²⁹ had 864 injection sites, and another for the HSCT program had 1152 sites.

The large increases in the number of fuel injection sites tend to determine the type of fuel injection system that might be used. The injector tip flow number (FN_{tip}) is defined as

$$\text{FN}_{\text{tip}} = (m_f)_{\text{tot}} / n \sqrt{\Delta P_f}$$

where n is the number of tips, $(m_f)_{\text{tot}}$ is the engine fuel mass flow rate, and ΔP_f is the fuel pressure drop across the tip. Because $(m_f)_{\text{tot}}$ and ΔP_f are fixed by the engine cycle and the fuel pump, the individual injector FN_{tip} decreases dramatically as the number of tips increases, even allowing for the increase in fuel line pressure losses. Because the atomization performance in terms of Sauter mean diameter (SMD) of a simplex pressure atomizer can be expressed as³⁰

$$\text{SMD} \sim \frac{(\text{FN}_{\text{tip}})^{0.205}}{(\Delta P_f)^{0.251}}$$

fairly good atomization (around 40–60 μm typically) can be achieved without the use of excessive fuel pump pressures. This allows the use of macrolaminate technology for inexpensive manufacture of the tips. Conventional airblast atomization can usually achieve SMDs around 20 μm or less at high-power conditions, but

is probably a prohibitively expensive technology for this use. A practical limitation occurs when the FN_{tip} fall below unity. Even with macrolaminate technology, it is extremely difficult to manufacture to narrow tolerances in flow number without excessive production rejection rates. Significant local deviations in fuel flow rate that result produce severe local changes in S , causing high NOx generation. Care also has to be taken in introducing the injector air to not collapse the fuel spray cones, particularly if some form of carburetor tube is used.

The use of very large numbers of injection sites necessitates the use of multiple stages within the main stage itself to ameliorate the typical increase in CO and UHCs at staging, such as seen in Fig. 14. This is because the fuel flow rate per individual site at staging would be excessively small if all sites were fueled simultaneously, resulting in ultralean combustion.

Data on the performance of LDI systems are largely still proprietary. The HSCT program LDI configuration from GE, which had 1152 main-stage injection sites and 48 injection sites in the pilot stage, demonstrated in rigs single-digit NOx emission indices at 17 atm pressure and 811 K air inlet temperature (supersonic cruise conditions). There was a very strong sensitivity of NOx to mixer tube fuel/air ratio, as might be expected from Figs. 17 and 18. (This system is only functionally an LDI combustor. Fuel is introduced into arrays of air tubes mounted in the combustor dome. For this reason, it has been described as a premixed system. However, the degree of premixing actually achieved is negligible, and therefore, for convenience, the system has been described as being LDI here. Strictly, it could more correctly be referred to as a partially premixed system.) In addition to the pilot, the main stage had five fuel staging modes to bring it up to full-stage fuel flow. Data from a NASA concept²⁹ that is not really engine-worthy have results that are not especially encouraging, although this is almost certainly due to the particular implementation rather than to the LDI concept itself. All of the combustor air passed through the dome, which had a substantial annular height to accommodate all of the 864 swirl-cup injection sites. Although the flame length was very short, coupling the dome to the turbine inlet height resulted in the existence of an extensive thermal soak zone. It would be expected, therefore, that NOx would correlate strongly with combustor exit temperature. Figure 20 shows that this is, indeed, the case.

Comparison of the NOx vs CO trade curve for this NASA LDI with that of the quasi-staged RQL combustor given originally in Fig. 14 suggests that this realization does not actually represent an emissions technology improvement. This is shown in Fig. 21. There are indications that the LDI trade curve might cross the quasi-staged

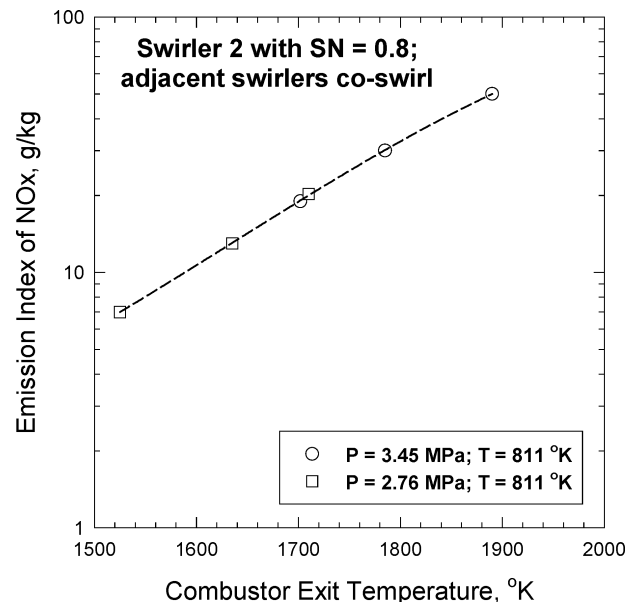


Fig. 20 NASA John H. Glenn Research Center LDI high-temperature NOx data related to combustor exit temperature.

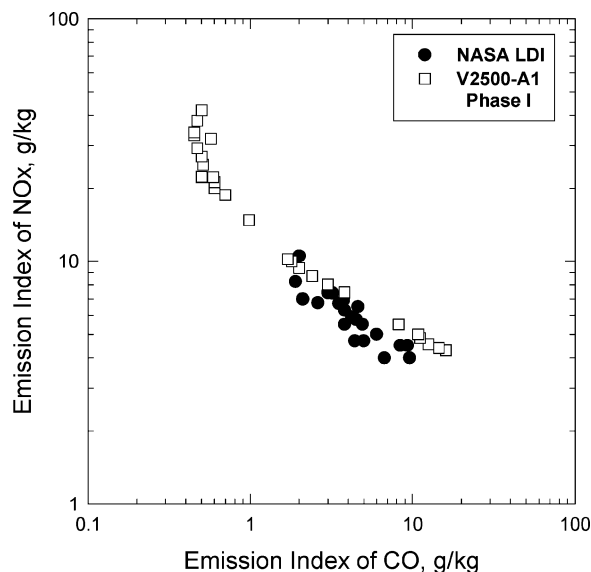


Fig. 21 Comparison of NASA John H. Glenn Research Center LDI emissions trade curve with a quasi-staged RQL trade curve.

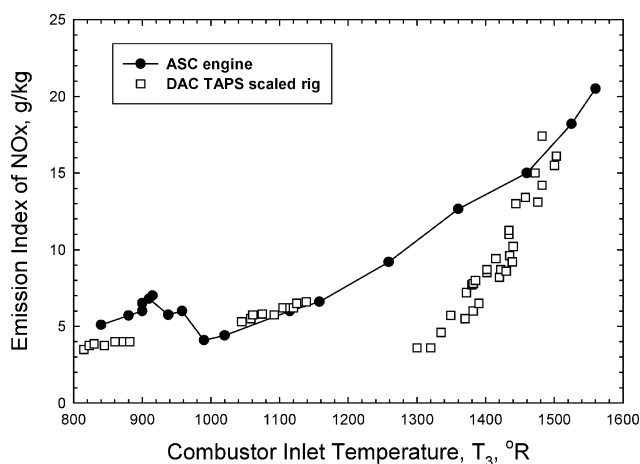


Fig. 22 NOx comparison up engine operating lines of GE DAC TAPS LDI concept with the ASC concept.

RQL trade curve. The major benefit appears to be lower NOx at low-power conditions. These LDI test data are sector-rig results.

Figure 22 shows a comparison of GE's twin annular premixing swirler (TAPS) LDI technology with the ASC engine NOx data. The TAPS LDI rig database was developed as functions of pressure, T_3 , and OFAR for each fuel staging mode, and the correlations were used to extend the data to an engine with an OPR of 30 (Ref. 31), which is appropriate also for the axially staged combustor (ASC) engine tests. The DAC TAPS combustor has a configuration like that of Fig. 12, with the substitution of the TAPS fuel injectors, which are of the type using a central pilot with staged secondary injection being arranged concentrically about each pilot to produce the flowfield shown in Fig. 23.³¹ The pilot/cyclone interaction zone is all important to this design. It is intended to allow the pilot flame to assist ignition and burning of the premixed flame. There are two design limits. One is when the pilot recirculation zone is fully merged with the premixing cyclone flame zone, that is, all interaction zone. The second is when the pilot recirculation zone is completely separated from the premixing cyclone flame zone, that is, zero interaction zone. For the first limit, experience teaches that the low NOx capability is lost or substantially reduced. For the second limit, two separate flame zones exist that can talk to one another, with potential acoustic problems. The secret to success is to get the interaction zone just right. All of the required airflow, with the exception of liner cooling air, can be passed through the dome with this approach to ensure lean operation of the cyclone stages, shown in Fig. 23. The

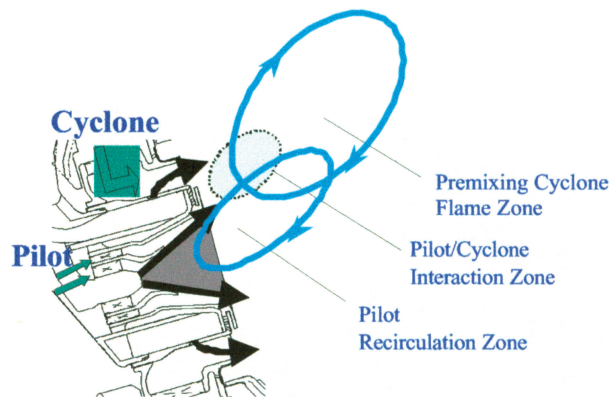


Fig. 23 GE TAPS LDI concept showing pilot, main and interaction burning zones.

TAPS data for simulated engine conditions are based on annular rig tests for OFARs to 0.037, combustor inlet temperatures T_3 to 1639°R, and pressures to 23.8 atm. No experimental uncertainties for the measurements were reported in the original GE paper.

The staging possibilities with the DAC TAPS design are somewhat flexible. It can be operated as a radially staged combustor, as in the existing DAC system, as a pilot/cyclone staging of all injectors of both banks, or as any combination of these. In addition, modulation as a function of engine power of the fuel split between pilot stages and cyclone stages provides further flexibility on NOx control. Actual staging mode and staging points for a given application would be determined by balancing emissions, operability, and fuel passage coking tendencies. Note that the DAC TAPS design has 30 fuel injector supports, each one mounting two tips. Within each tip there is a primary nozzle and a number of secondary nozzles, so that there are several hundred fuel sources altogether in the combustor. For the same air pressure drop as a conventional combustor, therefore, the DAC TAPS certainly achieves a lower value of the mixing parameter S than the standard DAC, although its values have not been assessed. Introducing all of the air through the dome reduces bulk equivalence ratio. Herein is the secret of the low NOx potential of the approach. Because the combustor was designed to be accommodated in the existing casing, there is no change in bulk residence times. This would not be the case though for a brand new design, however.

It can be seen from the Fig. 22 that the pilot stage of the DAC TAPS combustor has reduced NOx compared to that of the ASC. At T_3 around 800°R, 100% of the engine fuel flow is going to the TAPS pilots. Staging appears to take place at about 1160°R, which is much delayed in comparison with the ASC. However, the subsequent slope of the NOx curve is steeper than that for the ASC so that the two curves cross at about $T_3 = 1500^\circ\text{R}$. It is not immediately clear why the fully staged slopes are so different, but it is possibly associated with mixing differences. The potential benefits of multiple staging can be appreciated from Fig. 22.

Unfortunately, no CO data are available to allow construction of the NOx vs CO trade curve for the DAC TAPS combustor and to then allow comparison with the quasi-staged RQL trade curve as has been done for the other low-emissions concepts.

Situation Summary

Except for very high-temperature rise combustors, the nonequilibrium CO and UHC emissions result from incomplete combustion and are physically controlled. They can be addressed by attention to liquid fuel atomization, fuel placement, bulk stoichiometry adjustments in the combustor primary zone, and reduced dome and liner cooling air. Although CO and UHC can present serious problems for older engines, particularly where long ramp times are involved, they are much less of a problem with modern engines. NOx emissions constitute the major atmospheric concern and are much more difficult to deal with.

In terms of the international civil aviation organization (ICAO) landing and takeoff (LTO) integrated emissions parameter

D_p/F_{00} , NOx emissions are grouped by combustor design, specifically, by the emissions control technology incorporated in the combustor and its residence time. This is illustrated for some PW engines in Fig. 24 as a function of OPR using data obtained from the ICAO emissions databank. Engine data in the ICAO databank do not usually quote measurement uncertainties. However, the data reported are normally for three tests on a single engine, and the measurements are made with calibrated instrumentation and closely follow established EPA test protocols. The first group of JT9D data is for old combustors containing embryonic quasi-staged RQL reduced-emissions technology. The second group, involving the PW2000, PW4000 and IAE V2500 engines, are for modern design combustors (lower residence times, more effective aerodynamics reducing parasitic pressure losses) utilizing the quasi-staged RQL technology. The PW4000 Talon 2 combustor uses a refined version of the quasi-staged RQL technology and is conventional in appearance, as can be seen from Fig. 25. For all of these engines, the bypass ratio (BPR) ranges from 4.1 to 6.8 and is not a factor. Similarly, in Fig. 26 for GE's dual annular combustor (DAC) 1 and 2 technology in the CFM56 and GE-90 engines, where the BPRs range from 5.7 to 8.6, the NOx data group by combustor design.

If the engine data in Figs. 24 and 26 represent the current best standard of engine demonstrated reduced emissions technology, then these data in relation to the emissions regulations indicate the current low NOx status. The collected PW and GE data from Figs. 24 and 26 do group together, as is shown in Fig. 27, where they are compared with the ICAO Committee on Aircraft Environment Protection (CAEP)/4 standard (for OPRs greater than 30) adopted in 1999 for 2004 enforcement.

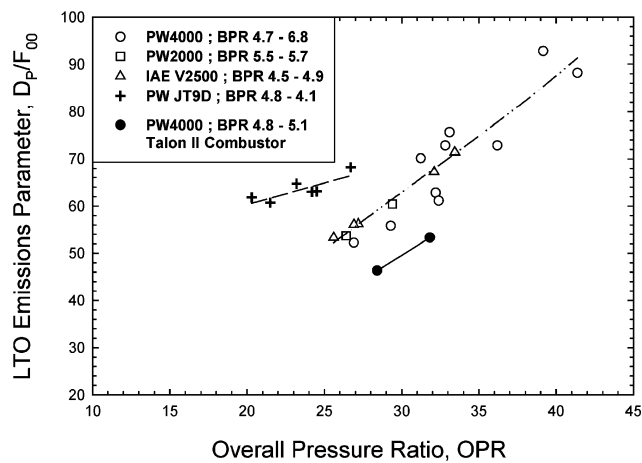


Fig. 24 PW's quasi-staged RQL NOx emissions technology.

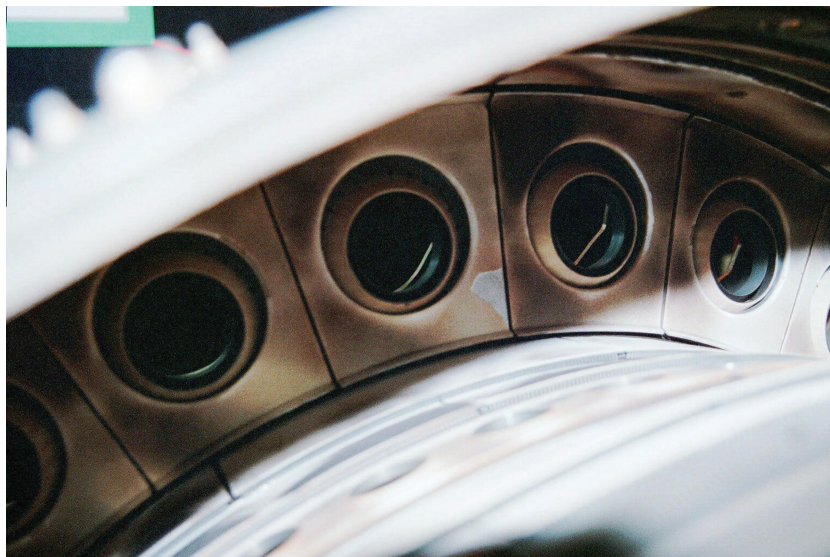


Fig. 25 PW Talon 2 combustor showing simplicity and conventional appearance.

Note that the level of low-emissions technology has projected NOx emissions that equal and exceed the CAEP/4 line for OPRs just over 50. Because carbon dioxide is now becoming to be considered as important as NOx in terms of its effects on the environment, and because fuel burn is reduced by increasing OPR and BPR, the trend of increasing OPR will be continued at least into the 50 level. Therefore, for future engines with increased OPRs, further improvements in combustor low-emissions technology over the current best

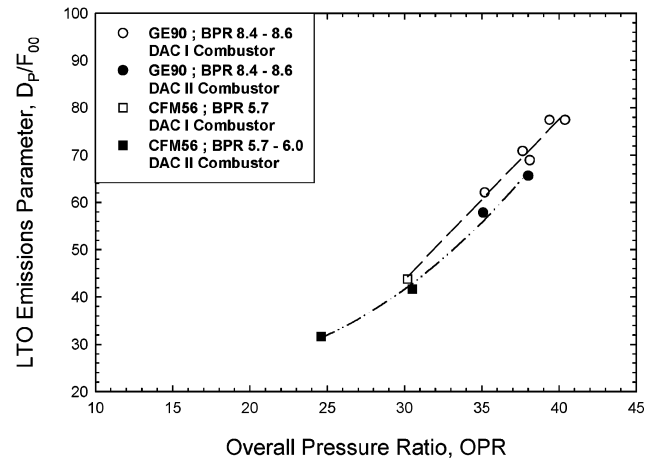


Fig. 26 GE's DAC 1 and 2 low NOx emissions technology.

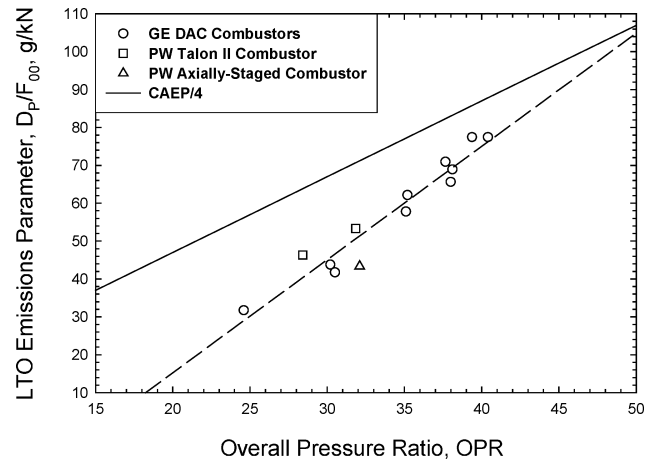
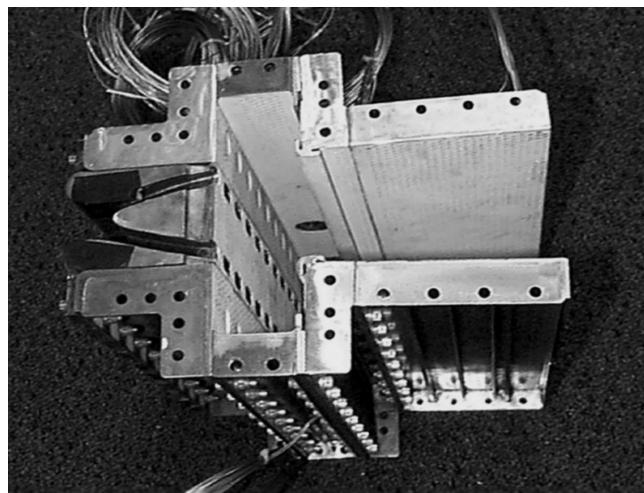
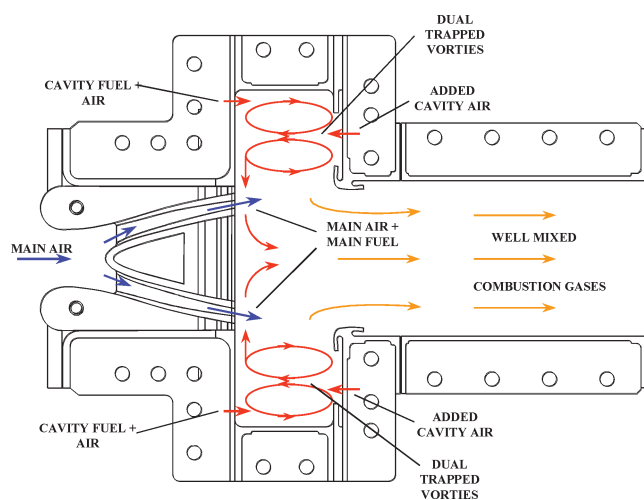


Fig. 27 Comparison of current engine low NOx technology with regulations.



a)



b)

Fig. 28 TVC: a) GE 12-in. planar-sector rig (two-passage diffuser) and b) schematic of TVC.

engine standard are going to be needed. TAPS-type technology, together with staging and reduced residence times, is a strong candidate. At the time of writing, recent verbal reports circulating in the industry suggest that PW's RQL technology in the form of the Talon-X combustor, which represents a further refinement of the Talon 2 combustor and has been explored under the NASA John H. Glenn Research Center Advanced Subsonic Technology/Ultra Efficient Engine Technology programs, has achieved additional and significant reductions in NO_x beyond the curve given in Fig. 28. It is apparently still a simple combustor, if less conventional in appearance than its predecessors. If this is so, then it is also a strong candidate.

The techniques for reducing CO and UHCs by recirculation zone changes have been introduced into service engines. GE's radially staged DAC combustion system is also in full commercial service. PW's ASC combustion system was engine demonstrated, but was not introduced into service. GE's DAC TAPS LDI combustor has been rig demonstrated. It requires some further work for CO and operability, and these issues are being actively worked. PW's Talon 2 and Talon-X combustors have been rig demonstrated and development continues.

Although it is really up to the original equipment manufacturers to assign appropriate technology readiness levels (TRLs) to their own low- or reduced-emissions approaches, some provisional assignments may be attempted based on the published information in the open literature. The NASA LDI has seen limited component testing and would be a TRL of 2 at best. The GE DAC 1 and 2 combustors have completed engine field service evaluations and are

in service and so would be TRL 8 or better. The TAPS LDI is in component testing and would be a TRL 5. PW ASC completed an engine demonstration and so would be a TRL 6; the Talon 1 and Talon 2 might be TRL 6 or higher, whereas Talon-X would still probably be a TRL 5.

U.S. Air Force Requirements and Considerations

The brief survey of the development of reduced-emissions combustors has revealed a story of steps forward, trades between emissions, and an ever-growing complexity in combustor hardware with consequent increases in cost and weight. The major difficulty is associated with NO_x reductions. Understanding of the details has grown tremendously, however. The issue of exhaust smoke has not been touched on here because it is worthy of separate treatment.

U.S. Air Force engine design requirements have traditionally stressed advanced performance in the form of increased thrust/weight ratio and specific thrust. Recently, affordability and life have also become issues of great importance. The combustor is expected to conform to previous design criteria, be fully affordable, and have long life with, now, the added concerns of exhaust emissions becoming important.

For engines to meet military design goals, combustors for fighter engines have always faced the issues of high-temperature rise and high combustor exit temperatures. Hand-in-hand with these have gone consequent reduced service intervals and high replacement costs. For future engines, if compression technology does not become limiting, high combustor exit temperatures are possible with only slight increases in temperature rise over current levels. Should compression technology become limiting, high combustor exit temperatures become essential, together with high-temperature rise. Clearly, these conditions imply turbine and combustor durability problems beyond those of today's engines. However, it is more complicated than this simple picture. High gas temperatures imply inherently high combustor exit NO_x levels, and as Fig. 17 demonstrates for high equivalence ratios, combustors that have good fuel/air mixing will have higher NO_x than combustors that have less perfect fuel/air mixing. Equilibrium chemistry allows dissociation of CO₂ to CO at such high temperatures, such that at an OPR of 35 the emission index of CO is 0.025-g/kg fuel burned for an exit equivalence ratio of 0.5 and is 15 g/kg for an exit equivalence ratio of unity. Treating the combustor as a perfectly stirred reactor with finite rate chemistry at a (cold) combustor residence time of 5 ms, the stoichiometric equivalence ratio of H₂/O₂ is reached for an exit equivalence ratio of 0.5, the stoichiometric equivalence ratio of C₂H₂/O₂ is reached at 0.9 exit equivalence ratio, and the stoichiometric equivalence ratio of CO/O₂ is reached at unity equivalence ratio. Because the high gravitational forces experienced by the gases exiting the combustor in flowing through the high-pressure turbine tend to concentrate cooler unburned gases and heavier molecules, significant combustion can take place in the turbine with the turbine and air-seal cooling air. Not only does this constitute a durability problem and increased pressure losses, it also implies further NO_x generation downstream of the combustor. These issues raise the question of whether or not future military combustors should have near-stoichiometric exit conditions. In other words, cycle performance might be traded for durability and reduced cost of ownership. The U.S. Air Force versatile affordable advanced turbine engine (VAATE) program is looking at the overall picture, which now involves not only performance, but also durability, emissions and affordability.

Clearly, the directions being pursued for low emissions in commercial engines are not completely consistent with U.S. Air Force design requirements, except for transport aircraft that use derivatives of commercial engines. Multiple injection sites and staging adds system weight and cost, whereas multiple-staging modes adds complexity and probably also has an adverse effect on reliability through fuel passage coking propensity. The thought of a low-emissions combustion system repeatedly staging and unstaging during combat maneuvers is disconcerting. Mechanically staged combustion systems, therefore, are most unlikely to be considered seriously for combat aircraft. It would seem prudent, therefore, that some alternative approaches for U.S. Air Force applications might be

advantageously considered in addition to pursuing TAPS/LDI technology. The Talon 2/Talon-X RQL technology is one approach that offers some possibilities here, provided smoke and particulates do not become serious issues from a stealth point of view.

Simpler Combustor Approaches for Military Applications

Trapped Vortex Combustor

A military combustor must have the best possible pilot to satisfy severe engine operability requirements. Most of the conditions for good pilot design have been described above. In all of the combustor designs discussed so far, the pilot recirculation zone that holds flame is exposed to the aerodynamically destabilizing influences of the main flow in one way or another. Therefore, it has to be substantial in size. The large size means long-residence times that contribute significantly to the total NO_x generated. Furthermore, smooth connection of the pilot with its large annular height to the turbine inlet results in the formation of thermal soak zones that also contribute to NO_x.

The trapped vortex combustor (TVC)³² was originally conceived as a high-performance (low-pressure drop, high-temperature rise) combustor specifically for advanced military applications. It also has the potential of reducing engine length, where in military engines 1 in. in axial length can be worth up to about 100 lbm in installed engine weight. A TVC mechanically anchors a pilot recirculation zone on a time-averaged basis by holding it within a specially designed cavity.³³ The cavity protects the recirculation zone from main-stage flows. The recirculation, therefore, can be smaller than a conventional recirculation zone, while having a superior operability performance.³⁴ The smaller recirculation region, through reduced residence time, offers the possibility of a less severe impact of the pilot on overall NO_x emissions. Furthermore, if the TVC is designed with its zones in parallel,³² that is, with the pilot being placed parallel to the main flow, the overall combustor length is further reduced. This saves weight and reduces the thermal soak zones for lower NO_x.

Figure 28a shows a GE-designed, TVC³⁵ planar-sector rig. The configuration shown is a staged combustor, where the main-stage fuel is introduced into the combustor two-passage diffuser section, which has been integrated to form the combustor dome to give another reduction in section length. The main stage forms an LDI. There are inner and outer cavities placed in parallel to the main stage that are separately fueled. In a generic sense, the hot combustion gases are recirculated within the cavity and are then extracted from it by the low-pressure wake regions formed by the mainstream flow from the diffuser passing through the combustor dome. An igniter plug is contained in the outer cavity; ignition of the inner cavity occurs by flame transport across the central bluff-body flameholder of the main stage. The downstream exit corners of the cavities are provided with film-cooling slots, and thermal barrier coating is applied to all surfaces. The main-stage flameholder and cavities have application of angled, multihole cooling passages for enhanced durability. The rig could be operated as a staged LDI combustor, or as a quasi-staged RQL combustor when only the cavities are fueled. Operating as a staged LDI, the overall flame length is extremely short. Emissions measurements indicate that the combustor shown in Fig. 28 could be shortened in exit length a further 40% without driving up CO. The section length of this concept in an engine is only a fraction of that of a conventional design.

Figure 28b shows the notional flow patterns described earlier. Note the double-vortex system formed in the cavities by means of mainstream flow over the cavity and the direct introduction of air jets into the cavity. Flow patterns in the cavity proved to be critical in determining performance. The vortex systems established proved to be remarkably stable in that flame movies shot at 12,000 frames/s still exhibited regular, vigorous, and tight recirculation zones fully contained within the cavities.

The performance of the TVC of Fig. 28 was extremely encouraging for a new concept when operated over a range of pressures from subatmospheric to 20 atm with a nonvitiated heated air supply on liquid JP-8+100 fuel. The static stability (LBO) was over twice

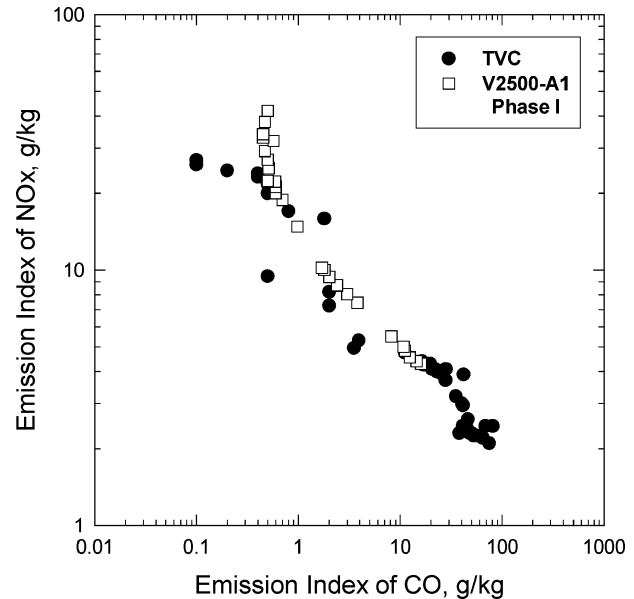


Fig. 29 NO_x vs CO trade comparison for TVC and quasi-staged RQL combustor.

as good as that of a conventional combustor at the same combustor loading over a wide range of loadings. Successful altitude relight was demonstrated up to engine conditions representative of over 20-km height, and stable combustion was maintained to conditions representative of greater than 40-km flight altitude. Propagation of flame from the outer cavity to inner cavity across the mainstream via the main-stage flameholder was satisfactory on starting. Without any dilution air jet assistance, combustor outlet temperature distributions (profile and pattern factors) were acceptable to a turbine, and operation at stoichiometric outlet conditions was successfully demonstrated. The combustion efficiency at idle conditions was in excess of 99%, and this was held over wide ranges of OFAR; the efficiency at the staging point was very high also, in excess of 99%.

When operating as a staged LDI device, the NO_x vs CO trade curve was moved closer to the origin compared to that for the GE-90 staged combustor shown in Fig. 14, thereby representing a truly reduced emissions device. Note that the initial main-stage injection system of this LDI was far from ideal, so further improvements in emissions could result from attention to the main-stage fuel system design. When operated as an RQL device (cavities only fueled), the NO_x vs CO trade curve moved even closer to the origin than that for the staged TVC, whereas NO_x levels were essentially the same as for the staged TVC. Figure 29 shows a comparison of the TVC NO_x vs CO trade curve to that for the quasi-staged RQL originally given in Fig. 15 and against which all subsequent concepts have been compared. It can be seen that the TVC emissions are either the same or slightly better than this standard. At very high OFARs, the TVC NO_x signature with engine power in the RQL mode became concave upward, and levels eventually exceeded those of the staged TVC. Although rig smoke numbers should always be viewed with care, the smoke decreased with increasing OFAR, indicating that the smoke originated in the fuel-rich cavities and was subsequently and progressively burned up in the main stage as this became hotter. Smoke levels at high-power conditions were less than 10.

It was surprising that the initial durability in the cavities where combustion is intense, and on the dome, was excellent, apart from the usual minor TBC loss on the dome. The multihole cooling used was industry standard and did not use excessive cooling air. Indeed, the cavity cooling air was also used to assist in driving the vortices. The double-headed film cooling slot on the downstream lips of the cavities suffered from the usual weaknesses of film-cooling slots and would need some redesign for engine application.

Although it has a novel configuration, the TVC appears to be a viable combustion device for aircraft applications. It certainly demonstrated its potential as a reduced length/weight-savings

high-temperature rise combustor with enhanced operability for military applications. In addition and without any specific attempt to design for low emissions, it achieved the best low-emissions potential of all of the simpler combustor concepts reviewed. A full annular rig demonstration is planned for the future. At the present stage of its development, the TVC would be a TRL of 2.

Ultracompact Combustor

The primary zone, where flame is stabilized and most of the total heat release is achieved, forms the heart of a combustor. A poorly designed primary zone will always result in a poorly performing combustor, regardless of how much effort is put into the intermediate and dilution zones and flow around the combustor. It is not surprising, therefore, that significant gains in reducing emissions have come from major changes to the primary zone, as in the inside-out recirculation (Fig. 4) and the TVC (Fig. 28). More aggressive versions of the TVC offer the dual possibilities of further emissions reductions through reduced mainstream residence times and additional reductions in engine length and, hence, in engine weight. One version of a more aggressive TVC has been named the ultracompact combustor (UCC). It is presently a research project only and is intended for feasibility studies. However, it does represent a continuation of the line of thinking that combustors can be shortened very considerably over existing designs with the use of nonconventional approaches. With a short length, of course, goes a reduction in thermal NO generation.

One UCC concept that is being explored experimentally combines the combustor with the compressor exit guide vanes (CEGVs) and the turbine inlet guide vanes.^{36,37} This concept utilizes a swirl-based trapped vortex, where the major axis of the swirl is the engine centerline, in addition to the minor axis of swirl generated by flow over a cavity normal to the major flow direction. Thus, the motion of reacting flow within the cavity, which is nominally set normal to the flow through the engine, follows a spiral motion around the engine centerline. Swirling flow combustors have long held the interest of designers for high-intensity combustion systems with the elimination of the CEGVs, for example in Ref. 38. The large centrifugal force field generated by the major swirl enhances combustion through high levels of buoyancy-driven turbulence.^{39,40}

It can be shown that burning velocity S_b is proportional to a swirl parameter,

$$S_b \propto (T_b/T_u)\sqrt{g}$$

where

$$g = w^2/g_0 r_{\text{cav}}$$

T_b and T_u are the burned and unburned gas temperatures, respectively, w is the swirl velocity in the cavity, g_0 is Newton's constant (where the units used might necessitate its inclusion), and r_{cav} is the mean radius of the cavity. A typical value of gravitational force for conventional, swirl-stabilized combustors is about 90, whereas values experienced in the UCC rig are estimated to range from 350 to 3500.

Figure 30 shows the UCC concept. It can be seen that in addition to the main cavity, the wide-chord vanes also have radial cavities that transport partially burned mixture out of the main cavity to complete combustion and distribute the hot gases across the main flow. An optional circumferential flameholder is shown, whose purpose is to distribute hot gases circumferentially and to complete any remaining combustion under adverse burning conditions. All combustion takes place in low-velocity flow regions and is completed before the gauge point of the cascade to avoid high Rayleigh losses. Functionally, the circumferential cavity serves as primary zone, the radial cavities serve as the intermediate zone and the optional circumferential flameholder serves as a dilution zone. Computational fluid dynamics (CFD) studies of the concept show flow behavior as postulated, with field responses to geometrical changes as expected. To control weight of the combined vane pack/combustor, and for cavity durability, the use of composite materials is anticipated.

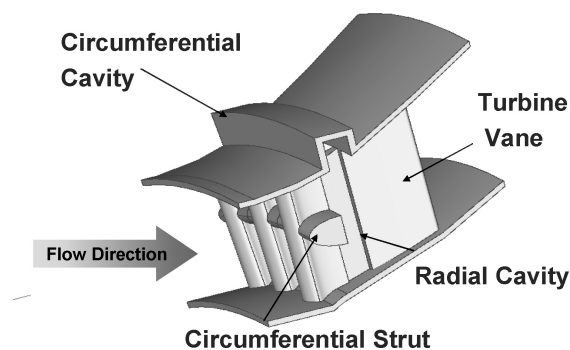


Fig. 30 UCC concept.

This UCC concept is too early in its development to permit any realistic comparisons of its emissions characteristics with the engine and developed rig combustor results presented earlier. Nonetheless, it is interesting to look provisionally at some of the emerging emissions behavior. A small rig is being used to study the main circumferential cavity at atmospheric pressure.³⁷

The initial rig consists of a small cavity mounted in the outer wall of a circular cross section duct that carries the main air. A number of air ports are positioned in the outer circumference of the cavity to provide separately metered combustion air with swirl around the cavity. All airflows are heated electrically to 500°F. The cavity contains six circumferentially disposed pressure atomizing fuel injectors, also mounted in the cavity outer circumference. The injector major axes can be changed from 0 deg (straight radial injection) to 37 deg off radial to give injection in the direction of the air swirl. The fuel is liquid JP-8+100. A centerbody is provided in the circular duct. This center-body is positioned by several thin support spiders upstream of the main cavity. Although not intended to function as simulations of the radial cavities of the concept, the low-pressure wakes from these spiders nevertheless do provide some mass transport from the main cavity. The major operating variables are mainstream velocity, air pressure drop across the cavity, and cavity equivalence ratio. The cavity equivalence ratios are in terms of the metered values. Because it is known that cavities such as this can entrain considerable quantities of mainstream flow, the actual cavity equivalence ratios will always be much less than the quoted values. The effects of buoyancy-driven turbulence on the combustion efficiency of the main cavity are discussed in Ref. 41, where many questions also remain to be answered.

Emissions results for two fuel injectors, C and D, are presented. Both injectors are pressure atomizers using Parker Hannifin's macrolaminate technology, with some integral supplemental injector air for an airblast contribution to the atomization. For the C injectors, the supplemental air was nonswirling with an effective area of 0.033 in². For the D injectors, the supplemental air was swirled clockwise relative to the tip face with a swirl number of 0.8 and an effective area of 0.0234 in². This swirling supplemental air generated a small tip recirculation zone. The injector flow numbers were in the range 0.7–0.9 pounds per hour (PPH)/(psi)^{1/2}. These small injector differences resulted in significant differences in performance.

To have an appreciation for the CO emissions of this UCC concept, it is necessary first to have a feel for the combustion efficiencies achieved. The circumferential cavity is capable of delivering very respectable combustion efficiencies. Combustion efficiency is normally expressed in terms of a primary zone loading parameter at various values of primary zone equivalence ratio. This form of presentation is used here, where combustion efficiencies from gas analysis are given in terms of a cavity loading parameter (LP), exponentially corrected to 400°K, at various metered cavity equivalence ratios, where

$$LP = m_{\text{tot}}/VP^{1.8}$$

and where

m_{Tot} = sum of fuel flow and cavity metered air, lbm/s

V = cavity volume, ft³

P = combustion pressure, atm

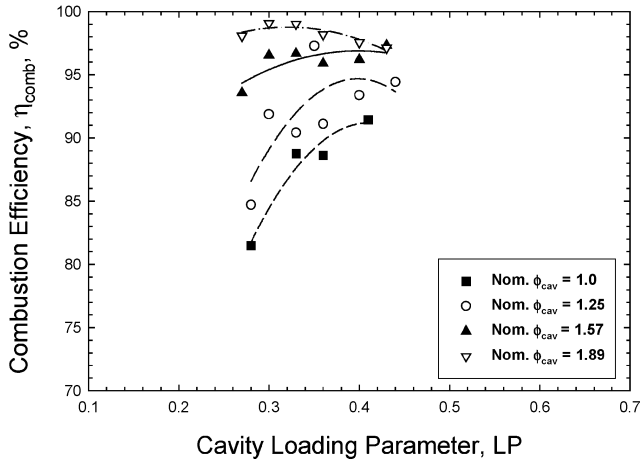


Fig. 31 Effect of cavity metered equivalence ratio on efficiency for D injectors at 20-deg injection angle.

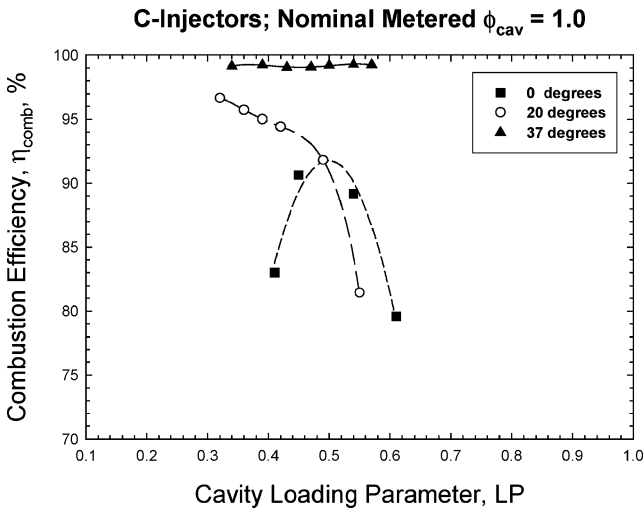


Fig. 32 Effect of injection angle on efficiency for C injectors at unity metered cavity equivalence ratio.

Figure 31 gives an example for the D injectors at 20-deg injection angle. Initially, efficiency grows as LP increases due to more effective swirl enhancing burning rates.⁴¹ After reaching a maximum value, it then falls due to increasingly inadequate residence time in the cavity as LP grows further. This falloff in efficiency begins at values of LP about 50–60% those for conventional combustors. The maximum levels of combustion efficiency increase with metered equivalence ratio ϕ_{cav} , and with increasing injection angle, as Fig. 32 shows for the C injectors. Under optimum conditions, the efficiencies are maintained at 99+% over acceptable ranges of LP.

NOx vs CO trades are presented in Fig. 33 at 0-deg injection angle for the C and D injectors over a range of ϕ_{cav} . The data for each injector group reasonably tightly and show no systematic dependence on ϕ_{cav} . Although each trade curve has the now familiar form, the differences for the two injectors are clearly apparent and result directly from the differences in combustion efficiency. (It would, of course, not be reasonable to compare this exploratory UCC rig data with the quasi-staged RQL engine trade data that has been made the standard of comparison in this paper.) The two injector trade curves cross, with the C injectors producing higher NOx at low CO than do the D injectors and, then, lower NOx at higher CO.

The effect of fuel injection angle on the trade curve for the D injectors is shown in Fig. 34, where going from purely radial injection to 37-deg angled injection shifts the curve to higher NOx levels. The effect of injection angle seen in Fig. 34 is again purely one of increased combustion efficiency, similar to that shown in Fig. 32 for the C injectors. However, the slope of the trade curve at the

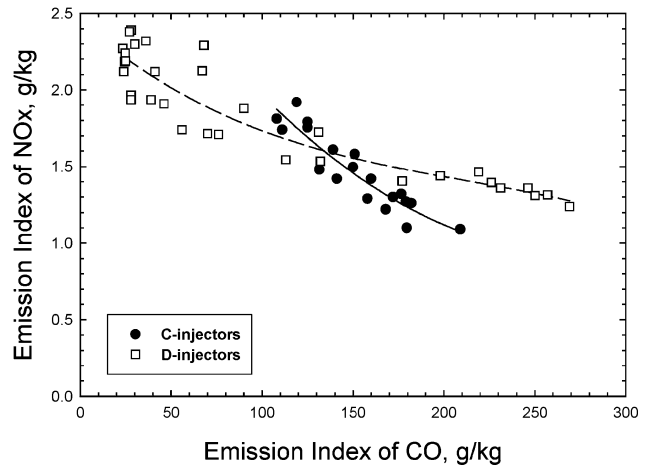


Fig. 33 NOx vs CO trade curves for C and D injectors at 0-deg injection angle: $1.0 < \phi_{cav} < 1.8$.

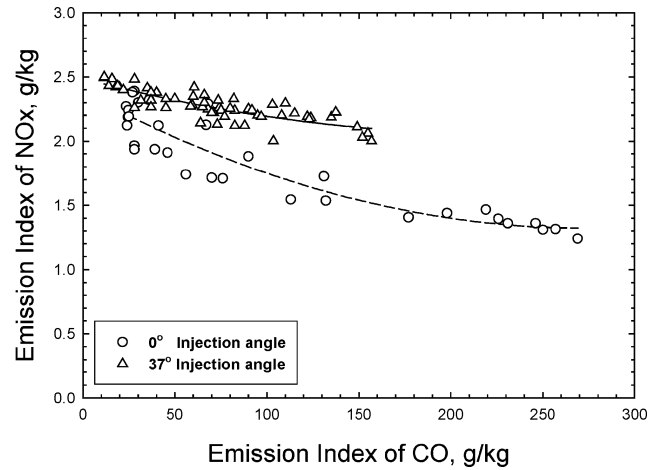


Fig. 34 Effects of injection angle on NOx vs CO trade curve for D injectors: all ϕ_{cav} .

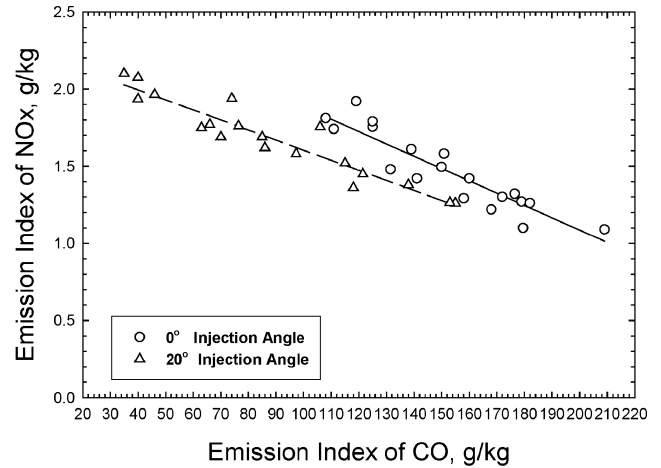


Fig. 35 Effects of injection angle in 0–20 deg range on NOx vs CO trade curve for C injectors: $1.1 < \phi_{cav} < 1.5$.

higher injection angle is less than that for radial injection. The data in Fig. 34 include all cavity equivalence ratios from unity to 1.8.

For the C injectors, the behavior of the NOx vs CO trade curves with injection angle is completely different than that for the D injectors. Figure 35 gives the trade curves for the C injectors at 0-deg injection angle for metered equivalence ratios in the range $1.1 < \phi_{cav} < 1.5$. At 20-deg injection angle when $\phi_{cav} > 1.5$, the correlation breaks down, and there is a systematic variation where individual curves exist for each equivalence ratio. This is believed to be

due to fuel burning outside of the cavity. Note that for the C injectors increasing the injection angle reduces the NOx.

For the C injectors at 37-deg injection angle, the relationship between NOx and CO breaks down into totally individual curves for each cavity equivalence ratio, as is shown in Fig. 36. For lean burning in the cavity (open symbols) the negative gradient of the curves increases with increasing metered cavity equivalence ratio until, for ϕ_{cav} equal to 1.16, NOx is virtually independent of CO. With allowance for entrainment of mainstream air into the cavity, this latter condition probably corresponds to stoichiometric burning within the cavity. The emission index of CO here is equal to about 15 g/kg. This considerably below the equilibrium value of CO for stoichiometric burning at 1 atm (137.9 g/kg); however, because the efficiency is not 100% and UHCs are present, and with the emissions measurement being taken downstream from the cavity in the mainstream, CO would be expected to be below this equilibrium level. As the lean-burning cavity equivalence ratios are increased, the individual curves move toward the ordinate of the graph, that is, a given NOx level is achieved at progressively lower levels of CO. The lower CO arises from the higher temperatures in the cavity. However, because the characteristic time for CO consumption is greater than the characteristic time for NO generation for lean burning, the gradients of the curves increase. At equivalence ratios slightly greater than unity, the characteristic times of CO consumption and NO generation become about equal.

For rich burning in the cavity (solid symbols in Fig. 36) the trade curves backtrack on themselves and become double valued. To understand this behavior, it is necessary to consider the constituent curves from which Fig. 36 is made up. Figure 37 shows the dependency of NOx on the cavity LP for metered cavity equivalence ratios

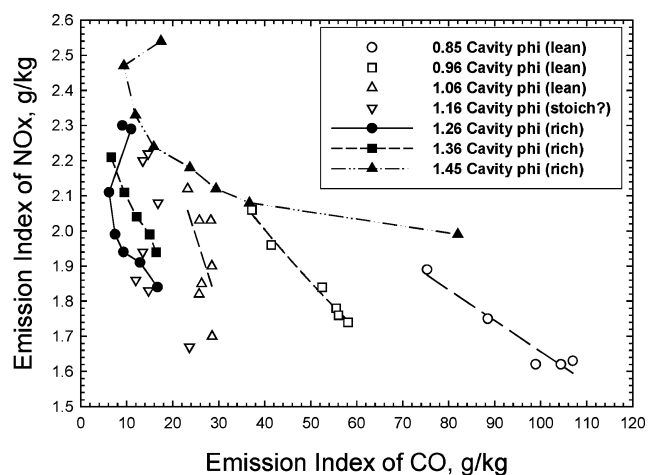


Fig. 36 NOx vs CO behavior for C injectors at 37-deg injection angle.

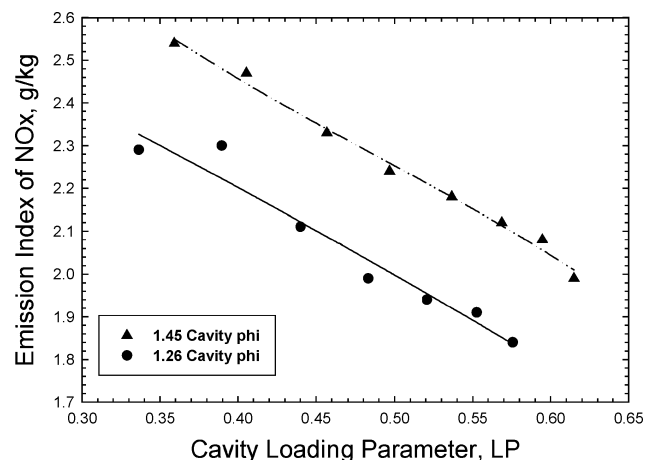


Fig. 37 Dependency of NOx on cavity loading for rich burning in cavity; C injectors at 37-deg injection angle.

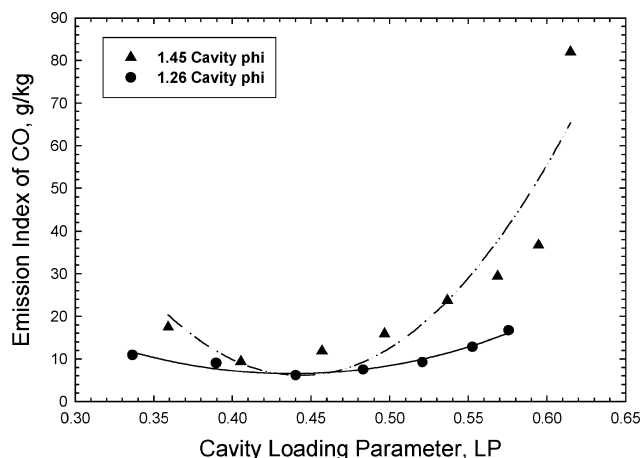


Fig. 38 Dependency of CO on cavity loading for rich burning in cavity; C injectors at 37-deg injection angle.

of 1.45 and 1.26; similarly, Fig. 38 shows the dependency of CO on LP at these equivalence ratios. LP is used here as the connector for consistency with the efficiency plots, Figs. 31 and 32.

Figures 37 and 38 show that NOx decreases essentially linearly with increasing cavity LP with increasing metered cavity equivalence ratio raising the levels of NOx and that CO varies in essentially parabolic fashion with increasing cavity LP with increasing metered cavity equivalence ratio raising the levels of CO, respectively. The minimum in CO is reached at about 0.44 cavity LP (units as given earlier) for both equivalence ratios, and the value of the minimum CO is around 10 g/kg. The characteristics of Figs. 37 and 38 explain the behavior seen in Fig. 33. Note that, for the lean-burning cases given in Fig. 36, NOx decreases for increasing LP with increasing metered cavity equivalence ratio raising the levels of NOx and that CO also increases for increasing cavity LP with increasing metered cavity equivalence ratio reducing the levels of CO.

The NOx behavior of Fig. 37 is explained by the decrease in cavity residence time associated with the increase in cavity LP and the NOx generated within the high-temperature cavity region. The initial decrease in CO of Fig. 38 is explained by an enhancement of burning rate in the cavity as the swirl is increased⁴¹ as cavity LP is increased. Eventually, however, the decrease in cavity residence time with further increases in LP overcomes the burning rate enhancement of increased swirl. There is then insufficient time at high temperatures to burn the CO, so that levels of it increase.

It can be appreciated that a detailed understanding of this combustor concept is still being worked on. More diagnostic evaluations of the behavior seen in Figs. 34–36, for example, are needed to comprehend fully the combustion behavior of the intensely swirling flow in the cavity. In the exploration of the behavior of the UCC, CFD is used as a tool in conjunction with experiment. An example of this use is given in Fig. 39, where the objective was to study mass extraction from the circumferential cavity by the radial strut wakes. In this instance, there are six fuel injectors equally disposed around the main cavity circumference and six non-turning struts, which are placed inline with the fuel injectors. The fuel injectors are angled at 38 deg off-radial and are positioned midway between pairs of angled air jets that generate circumferential swirl around the main cavity. The struts themselves have an angled cavity on the downwind side of the strut. The strut cavity is angled at 45 deg off the vertical from strut tip to hub; at the strut tip the strut cavity is aligned with the forward face of the circumferential cavity. Although the wire frame is a little difficult to interpret, the view is from the rear, and the strut with its cavity can be seen. Figure 39 shows a single fuel injector sector with its two pairs of air jets and the associated strut. It gives contours of gas temperature at two planes across the fore-and-aft cavity width. The first plane is taken through the centerline of the upstream of a pair of air jets, and the second plane is taken through the centerline of the fuel injector. It can be seen from Fig. 39 that

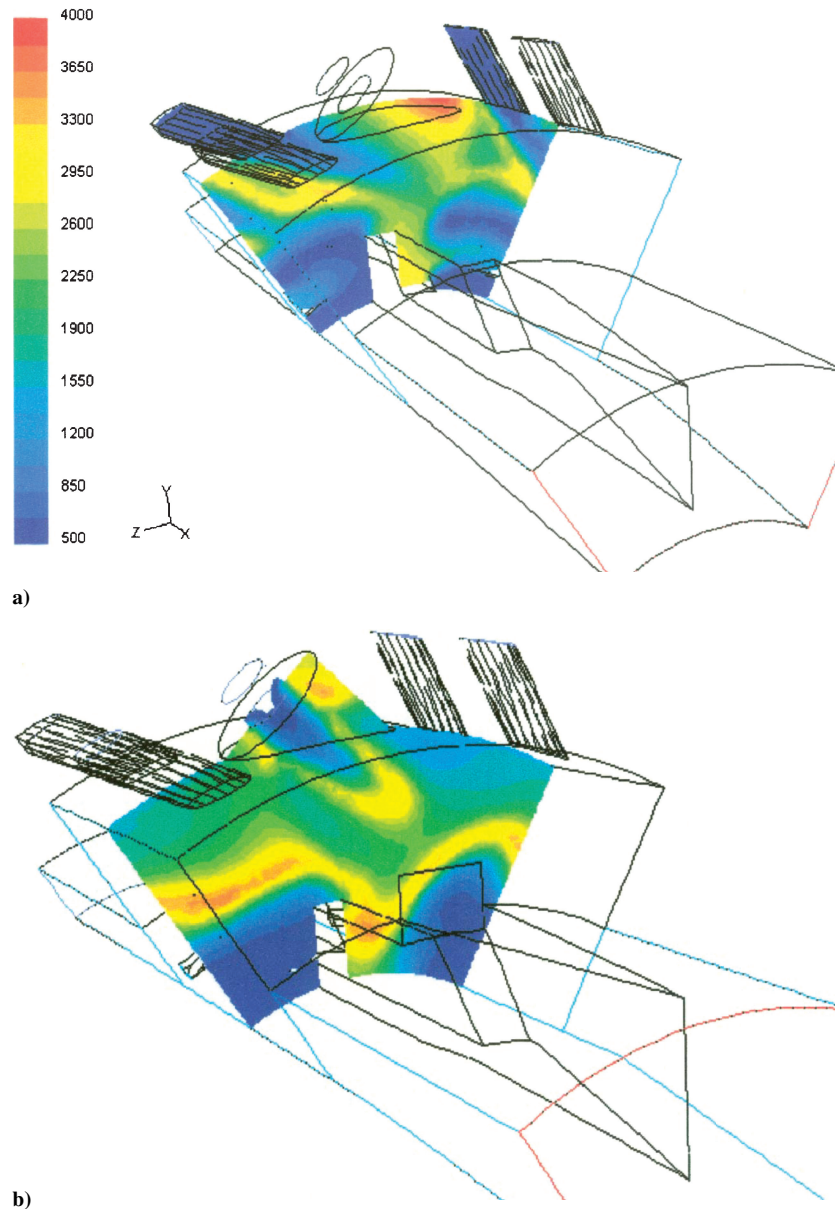


Fig. 39 CFD of UCC research rig; isotherms that reveal mass extraction from the circumferential cavity into radial strut cavities: a) inline with air jets and b) inline with fuel injectors.

hot gas is drawn from the circumferential cavity into the strut cavity, even in the upstream plane, and that this process is continued and strengthened in the injector plane, which is only a small distance downstream from the first plane. This mass extraction by the strut cavity, of course, is the design intent. The motion of mass from the circumferential cavity to the strut cavity is generated by the static pressure difference existing between the two cavities. It is the motion of the mainstream by the strut cavity that creates the necessary low wake pressures to drive the flow from the circumferential cavity. Note that the existence of a significant radial velocity component in the mainstream flow is sufficient to overcome the effects of the pressure difference between the circumferential cavity and the strut radial cavity and, thereby, inhibit mass transfer out of the circumferential cavity. Therefore, outward cant angles (away from the engine centerline in the downstream direction) to the ASC must be avoided.

Although the purpose of these particular CFD studies was to explore the strut cavity design, it can be appreciated that the regions of high temperature shown in Fig. 39 would also result in high rates of nitric oxide generation, $d[\text{NO}]/dt$, and that the CFD tool can also be used for the purpose of minimizing NO by reducing regions of high temperature and by reducing the residence times within such regions. Experimental investigation of the effect of the radial struts and their cavities is currently in progress.

Clearly, the UCC concept itself is at a very early stage of exploration (TRL 1), and much remains to be done to understand the behavior, to formulate design rules, and to develop a reliable combustor. If these tasks can be accomplished, the low-emissions potential appears to be promising. When it is considered that only the functional primary zone of the concept, that is, the circumferential cavity, has been run experimentally thus far, a promising start can be said to have been made; again, much more remains to be accomplished. If the effort is successful, the potential weight savings in a military engine are likely to be considerable so that the effort is well worthwhile.

Engine Thermodynamic Cycle

The formulation of the ICAO emissions regulations are such that engine fuel burn plays an important role in the integrated emissions. Thus, a rather mediocre low-emissions combustor concept, if placed in a really efficient engine, can, in fact, satisfy the regulations with adequate margins. Therefore, the engine cycle itself can be a powerful tool in the effort to reduce emissions. Reduction in fuel burn with the Brayton cycle translates into a requirement for higher OPRs, increased BPRs, and higher fuel/air ratio combustors. The aircraft gas turbine is mounted in a moving vehicle so that the

overall efficiency is a product of the propulsive and thermal efficiencies. The most practical way to increase overall efficiency is to increase propulsive efficiency by reducing the exhaust jet velocity. This may be done by increasing BPR. The use of higher peak temperatures in the core engine allows higher OPRs without a falloff in thermal efficiency, as well as increasing thermal efficiency directly. Combustion at high pressures with consequently high air inlet temperatures and high turbine inlet temperatures together with higher combustor exit temperatures makes control of NO_x much more difficult. The high temperatures also increase engine material maintenance costs substantially.

The difficulties described arise in part because all of the heat release takes place in a single stage. A gas turbine engine has been proposed that uses a constant temperature (CT) cycle and intraturbine combustion such that gases enter the low-pressure turbine at the same temperature as they enter the high-pressure turbine. This allows large amounts of power extraction to be made from the low-pressure turbine for a variety of purposes.^{42,43} A variant of the CT cycle is the near-CT (NCT) cycle, in which second-stage combustion is confined to the inter-turbine duct between the high- and low-pressure turbines⁴⁴ for two-shaft engines. The cycle is not really new and has been known since the 1950s, but there are many difficulties in the way to achieving such an engine, although one model has been built and sold for ground power generation.⁴⁵

Such a NCT engine has been dubbed the interturbine burner (ITB) engine. High levels of low-pressure turbine energy are achieved with only a modest temperature rise across the ITB, and with reduced maximum temperatures in the engine when compared to the equivalent power Brayton cycle engine. Clearly, reducing the maximum temperature in an engine lowers its thermal efficiency, and so the ITB engine is better for some applications than others. Some examples that have been identified are some supersonic cruise applications; those applications requiring modest thrust augmentation, where a conventional afterburner might be otherwise required; and military applications demanding generation of large amounts of electrical power, where a special purpose auxiliary engine might otherwise have to be carried. Note that many commercial applications are now facing similar difficulties where the growing electrical power-generation requirements can cause near-continual operation of the auxiliary power unit, which is also a source of exhaust emissions. An example of another military application where large amounts of power extraction are needed for short periods of time is to drive a lift fan for standard takeoff and vertical landing operations. For most subsonic commercial applications, the NCT cycle engine does not even approach competitiveness with the Brayton cycle engine until very high OPRs (greater than 40) and ultrahigh BPRs (greater than 10) are used. The use of ultrahigh BPRs improves the propulsive efficiency and tends to make up for the reduction in thermal efficiency.

For specific thrust to be maintained, no increases in an ITB engine length can be allowed. Therefore, the ITB itself must be exceedingly compact. The UCC discussed earlier is a possible combustor concept for an ITB engine, being considered for both the main and interturbine combustors. There are two benefits to the ITB engine. The lowered peak temperatures improve engine durability, and they offer the possibility of reduced NO_x.

One ongoing study⁴⁶ to assess the NCT cycle and to evaluate the combustion possibilities has been applied to a future, large (65,000-lbf class) long-range transport, geared-turbofan two-shaft engine of ultrahigh BPR and high OPR, where an ITB engine sized to thrust for a particular mission profile is being compared to the equivalent advanced Brayton cycle engine. The two engines were designed to thrust and matched in OPR and specific thrust at the aerodesign point (36,000 ft, 0.85 flight Mach number). This matching favors ITB engine durability and low exhaust emissions over fuel burn, and the two engines can have a common nacelle that favors fuel burn for the Brayton cycle engine. At sea level static conditions, the OPR was 45.8 and the BPR was 22. With reference to Fig. 28, it can be seen that at this OPR the current generation of low NO_x combustors could not meet the CAEP/4 regulation for NO_x with sufficient margin (industry practice of 20%) for single-engine certification.

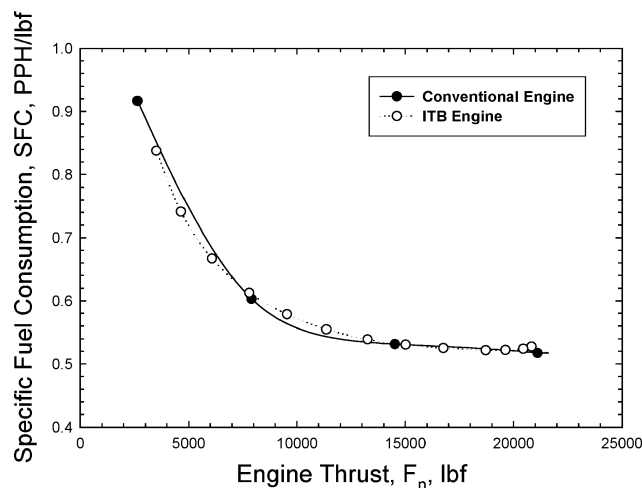


Fig. 40 Comparison of part-power specific fuel consumption for the Brayton and NCT cycle engines at initial cruise: initial cruise point 31,000 ft; and 0.85 M_0 .

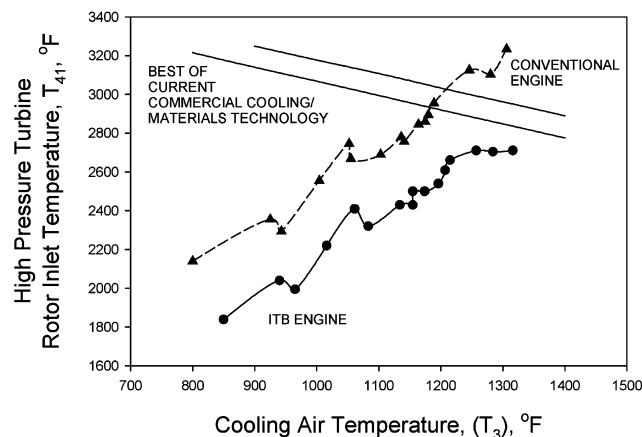


Fig. 41 Durability assessment for high-pressure turbine of the Brayton and NCT cycle engines around mission profile.

A comparison of the specific fuel consumption for the two engines at the initial cruise point is given in Fig. 40, where it can be seen that at this flight condition there is essentially no difference in part-power performance between the two engines. However, with the design choices imposed on the ITB engine for the comparison, the fuel burn for this very long-range mission of 7000 n miles unrefueled with complete crew of 21 plus their baggage, usual fuel reserves and 180,000 lbm of payload was +3.6% that of the baseline Brayton cycle engine. Relaxation of the common nacelle requirement would allow the ITB engine to utilize a higher BPR and, thus, reduce its fuel-burn penalty.

Figure 41 enables a durability assessment to be made for the expensive high-pressure turbines of the two engines from their installed performances. The temperatures given are around the entire mission profile. Note that the advanced Brayton cycle engine would severely challenge the best of current turbine blade cooling/materials technology, whereas the ITB engine would be more than satisfactory with 1990s technology.

The main combustor temperature rise requirements around the mission profile for the two engines, and for the ITB combustor, are given in Figs. 42 and 43, respectively. It can be seen that the main combustor of the ITB engine has a very easy task compared to that of the Brayton cycle engine, where the respective maximum temperature rises are 1500°F vs 2020°F. The ITB engine interturbine combustor has a maximum temperature rise of only 640°F at takeoff power; it is severely throttled back at cruise to only 185°F to minimize fuel-burn penalties. (Ideally, it should be shut down completely, but this would necessitate either a variable area

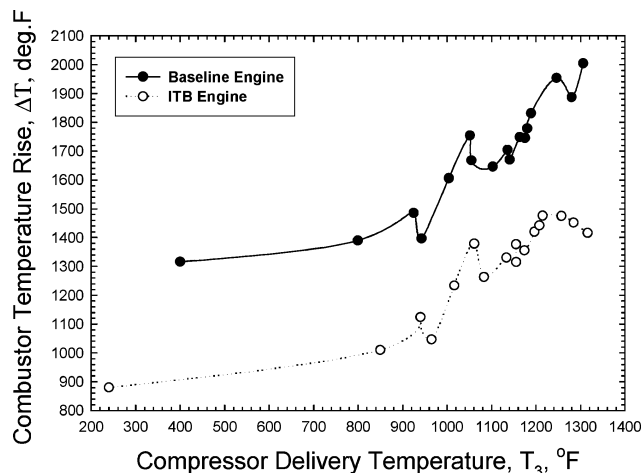


Fig. 42 Comparison of required temperature rise for main combustors of Brayton and NCT cycle engines around mission profile.

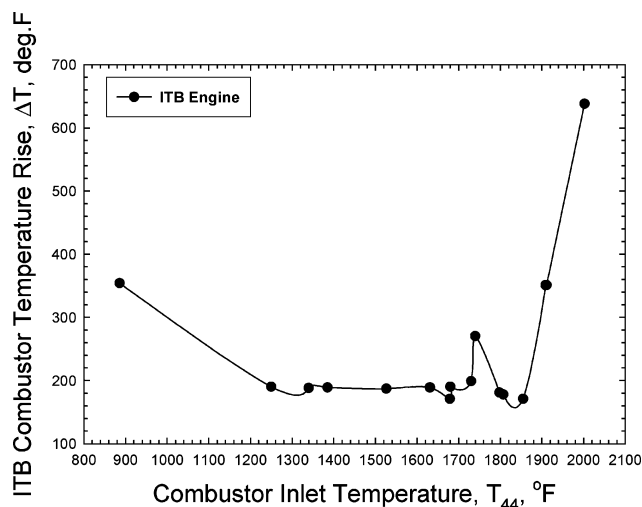


Fig. 43 Temperature rise requirements for interturbine combustor in NCT cycle engine around mission profile.

low-pressure turbine or a variable area propelling nozzle for the core engine.)

At takeoff (rotation), the maximum main combustor inlet temperature T_3 was 1316°F and the exit temperature T_4 was 2710°F; at the same conditions the inlet temperature to the ITB, T_{44} , was 2002°F and the exit temperature T_{45} was 2640°F. The combustion pressure for the main combustor, P_4 , was 853 psia, whereas the ITB combustion pressure P_{45} was 214 psia. With the modest temperature rise requirements given in Figs. 42 and 43, these are not especially severe conditions to design combustors for, and these combustors should not be severe NOx producers. For the baseline engine, the equivalent main combustor inlet and outlet temperatures were 1306 and 3310°F, respectively, and the combustion pressure was 825.5 psia. To get a general feel for the magnitude of the impact of these temperatures on possible NOx, consider Fig. 20 for the NASA John H. Glenn Research Center LDI combustor. The Brayton cycle baseline engine combustor exit temperature of 2094 K would indicate, with extrapolation, a NOx EI of around 100 g/kg, compared to a NOx EI of around 20 g/kg (interpolation only) for the ITB main combustor at its exit temperature of 1761 K.

Note that it was difficult to achieve a suitable engine flowpath for this two-shaft ITB engine. The rotational speed of the fan was so low that the booster compressor, which rotated at the same speed as the fan, had either very small annular passage heights in a conventional arrangement, or had too many stages if it was arranged inboard and parallel with the fan. A three-shaft engine would be a preferable layout. A three-shaft engine, with its three turbines, would also offer the possibility of using two ITB combustors. The use of two

ITB combustors is a thermally improved approximation to the ideal CT cycle engine.

The ITB engine and combustor concepts like the UCC that might help to make the ITB engine possible for some applications are both a long way from being made service-ready. They are included here to indicate some of the kinds of innovative thinking that are going to be necessary to continue the advancement of the combustion art in the face of ever-more demanding and restrictive design requirements.

Water injection also offers the possibility of Brayton cycle modifications to reduce takeoff NOx (Ref. 47). In this instance, rather than direct injection into the combustor as discussed earlier, water would be injected into the engine compression system. Through evaporation of the water spray, this gives a cooled compression process that reduces the amount of work that has to be extracted by the turbines to drive the compressors. For a constant thrust, therefore, the peak temperatures in the engine can be reduced. The mass of the injected water provides some thrust augmentation potential, so that again, for constant thrust, the peak temperatures can be lowered further. The combination of a cooled compression and reduced peak temperatures provides for a worthwhile NOx reduction. A system might be devised where this type of water injection could be used for NOx control during takeoff and where a low emissions combustor design without water injection is optimized for low NOx at altitude cruise conditions.

Again, the reduction in maximum temperatures for a constant thrust condition with cooled compression from water injection represents a reduction in engine thermal efficiency, and this could infer a specific fuel consumption issue. However, the time of water injection would only cover aircraft takeoff, climbout, and initial climb at most. Therefore, any fuel-burn penalties might not be severe. If combined with a low-emissions burner for low NOx at altitude, the injection of significant quantities of water into the compressor might exert some adverse effects on the combustion process, the magnitude of which would depend on the type of low-emissions combustor used. These could include local flame extinctions and increase in particulates. An additional concern where high stage loadings are used in the compression system, is the possible effect of water injection on movement of the operating line closer to the stall line for the compressor. Water injection requires careful consideration before implementation should be considered.

Summary

Control of engine exhaust emissions has become a leading design requirement of combustion equipment for aircraft gas turbine engines. It is an absolute requirement for commercial engines where compliance has to be demonstrated for certification. For military engines, it is becoming increasingly important even during peacetime, where aircraft operations and deployments can be affected through compliance with the NAAQS. The issue of direct emissions control in military engines will be addressed through the VAATE program. The story of reduced emissions combustors is one where progress has been made through coming to understand the root causes of pollutant generation. Emissions of CO and UHCs have proved relatively easy to control; NOx was harder, but progress has been made, albeit at the expense of an ever-growing complexity, cost, and weight of the combustion system. These developments are contrary to the desires of military engine designers, to whom thrust/weight ratio and specific thrust are vital issues. The complexity of these systems also adversely affects the cost and durability, and affordability is of growing importance to the military as well as to commercial operators. NOx generated by aircraft has emerged as being the really serious pollutant of the three gaseous emissions produced by aircraft gas turbine engines. The early successes in emissions reduction have resulted in a progressive lowering of the regulatory bar for this pollutant for commercial applications. However, the easy things in NOx reduction have all been done, and the way ahead requires more than incremental technology for continued successes. It appears as though more radical thinking beyond incremental technology may well be needed to meet the challenges presented in NOx reductions, especially for military applications. The regulations are now pressing low NOx technology to the point where changes to

the thermodynamic cycle are being thought about seriously for the future.

The issues of exhaust smoke and the particulates that make it up, together with the effects of contrails, have not been discussed here. However, they are growing in importance and are likely to receive increasing attention in the future, thereby exacerbating the difficulties of low-emissions combustor design.

The reduced emissions technology developed for commercial engines appears to be driven by NO_x considerations into systems that, by and large, are becoming ever more unsuitable for direct application to combat aircraft through their increased weight, cost, reliability, and operability penalties. Emissions reduction for such military applications can certainly borrow some of the commercial engine technology, but becomes very challenging for achieving low NO_x. Radical thinking in low-emissions design combustors will be needed, as well as some consideration of possible cycle trades, to satisfy the military application.

Acknowledgments

Part of this work is supported by Air Force Office of Scientific Research (AFOSR) with Julian Tishkoff serving as program manager, and we express our appreciation to J. Tishkoff for his courage, foresight, and enthusiasm. Another part of the work is supported by U.S. Air Force Contract F33615-01-C-2133 with J. Zelina as program manager. Hukam Mongia of General Electric was kind enough to make available to us a prepublication copy of his paper, AIAA Paper 2003-2657. Parts of this paper were extracted from Ref. 45, and the authors wish to thank C. Pellerin from the Strategic Environment Research and Development Program Office for his support. The authors wish to thank their colleagues in the U.S. Air Force and the industry for their many direct and indirect contributions over the years to this work.

References

- Robinson, A. B., Baliunas, S. L., Soon, W., and Robinson, Z. W., "Environmental Effects of Increased Carbon Dioxide," Oregon Inst. of Science and Medicine, Cave Junction, Oregon and George C. Marshall Inst., Washington, DC, Jan. 1998.
- "Ten Thousand Cloud Makers," editorial, *Science News*, Vol. 150, 6 July 1996, pp. 12, 13.
- Earth Science: "What Aircraft Leave Behind," editorial, *Science News*, Vol. 154, 18 July 1998, p. 47.
- Ballal, D. R., and Zelina, J., "Progress in Aero Engine Technology (1939-2003)," *Journal of Aircraft*, Vol. 41, No. 1, 2004, pp. 43-50.
- Lewis, J. S., and Niedzwiecki, R. W., "Aircraft Technology and Its Relation to Emissions," *Aviation and the Global Atmosphere*, Cambridge Univ. Press, London, 1999, Chap. 7.
- Blust, J. W., Ballal, D. R., and Sturgess, G. J., "Emissions Characteristics of Liquid Hydrocarbons in a Well-Stirred Reactor," *Journal of Propulsion and Power*, Vol. 15, No. 2, 1999, pp. 216-223.
- Sturgess, G. J., McKinney, R. G., and Morford, S. A., "Modifications of Combustor Stoichiometry for Reduced NO_x Emissions from Aircraft Engines," *Journal of Engineering for Gas Turbines and Power*, Vol. 115, No. 3, 1993, pp. 570-580.
- Sturgess, G. J., "Combustor Design Trends for Aircraft Gas Turbine Engines," American Society of Mechanical Engineers, ASME Paper 96-TA-29, June 1996.
- Sturgess, G. J., "Advanced Low-Emissions Catalytic Combustor Progress," Phase 1 Draft Final Rept. PWA-5587, Pratt and Whitney, East Hartford, CT, May 1979.
- Sturgess, G. J., "An Account of Fuel/Air Unmixedness Effects on NO_x Generation in Gas Turbine Combustors," *Intersociety Engineering Conference on Energy Conversion*, Paper IECEC-98-353, Aug. 1998.
- Sturgess, G. J., "Lecture Notes on Advanced Aircraft Engine Design, Vol. II—Engine Combustion and Emission Reduction," *Advanced Engine Design Workshop*, Inst. of Aeronautics and Astronautics, National Cheng Kung Univ., Tainan, Taiwan, Republic of China, 1994.
- Washam, R. M., and Mellor, A. M., "Emissions Correlations for Conventional Gas Turbines," EPA Grant No. R-804443-01—Final Report, Purdue Univ., Rept. PURDU-CL-77-06, Lafayette, IN, Dec. 1977.
- Takahashi, F., Switzer, G. L., and Shouse, D. T., "Structure of a Spray Flame on a Production Engine Combustor Swirl Cup," *Proceedings of the Twenty-Fifth International Symposium on Combustion*, Combustion Inst., Pittsburgh, PA, 1994, pp. 183-191.
- Lefebvre, A. H., *Gas Turbine Combustion*, McGraw-Hill, New York, 1983, Chap. 11.
- Tuthill, R. J., Madden, T. J., Craig, H., and Tuthill, R. S., "Combustor Bulkhead with Improved Cooling and Air Recirculation Zone," Patent 6,164,074 issued 26 Dec. 2000.
- Hedman, P. O., Sturgess, G. J., Warren, D. L., Goss, L. P., and Shouse, D., "Observations of Flame Behavior from a Practical Fuel Injector, Using Gaseous Fuel in a Technology Combustor," *Journal of Engineering for Gas Turbines and Power*, Vol. 117, July 1995, pp. 441-452.
- Switzer, G., Sturgess, G. J., Sloan, D., and Shouse, D., "Relation of CARS Temperature Fields to Lean Blowout Performance in an Aircraft Gas Turbine Generic Combustor," AIAA Paper 94-3271, July 1994.
- Bahr, D. W., "Technology for the Design of High Temperature Rise Combustors," *Journal of Propulsion and Power*, Vol. 3, No. 2, 1987, pp. 179-186.
- Fenimore, C. P., "Formation of Nitric Oxide in Premixed Hydrocarbon Flames," *Proceeding of the Thirteenth International Symposium on Combustion*, Combustion Inst., Pittsburgh, PA, 1971.
- Melconian, J. O., *The Design and Development of Gas Turbine Combustors*, Vols. 1 and 2, Northern Research and Engineering Corporation, Woburn, MA, 1980.
- Gogineni, S., Shouse, D., Frayne, C., Stutrud, J., and Sturgess, G. J., "Combustion Air Jet Influence on Primary Zone Characteristics for Gas Turbine Combustors," *Journal of Propulsion and Power*, Vol. 18, No. 2, 2002, pp. 407-416.
- Lohman, R., Pratt and Whitney, East Hartford, CT, 1996.
- Pandalai, R. P., and Mongia, H. C., "Combustion Instability Characteristics of Industrial Engine Dry Low Emission Combustion Systems," AIAA Paper 98-3379, July 1998.
- Segalman, I., McKinney, R. G., Sturgess, G. J., and Hung, L.-M., "Reduction of NO_x by Fuel-Staging in Gas Turbine Engines—A Commitment to the Future," *Fuels and Combustion Technology for Advanced Aircraft Engines*, CP-536, AGARD, 1993.
- Hassa, C., Carl, M., Frodermann, M., Behrendt, T., Heinz, J., Rohle, I., Boehm, N., Schilling, T., and Doer, T., "Experimental Investigation of an Axially Staged Combustor Sector with Optical Diagnostics at Realistic Operating Conditions," *Gas Turbine Engine Combustion, Emissions and Alternative Fuels*, RPT-MP-14, NATO Research and Technology Organization, June 1999.
- Brehm, N., Schilling, T., Mack, A., and Kappler, G., "NO_x Reduction in a Fuel Staged Combustor by Optimization of the Mixing Process and the Residence Time," *Gas Turbine Engine Combustion, Emissions and Alternative Fuels*, RPT-MP-14, NATO Research and Technology Organization, June 1999.
- Segalman, I., Smith, R., Sturgess, G. J., Morford, S., and Hoke, J., "Engine Demonstration of NO_x Reductions with a Fuel-Staged Gas Turbine Combustor," AIAA Paper 94-2712, July 1994.
- Heywood, J., and Mikus, T., "Parameters Controlling Nitric Oxide Emissions from Gas Turbine Combustors," *Atmospheric Pollution by Aircraft Engines*, CP-9-13, AGARD, April 1973.
- Tacina, R., Wey, C., Laing, P., and Mansour, A., "Sector Tests of a Low-NO_x, Lean-Direct-Injection, Multipoint, Integrated Module Combustor Concept," American Society of Mechanical Engineers, ASME GT-2002-30089, June 2002.
- Simmons, H. C., "Empirical Formulas (*sic*) for Prediction of Spray Drop Sizes," Parker-Hannifin Rept. 1966.
- Mongia, H. C., "TAPS—A 4th Generation Propulsion Combustor Technology for Low Emissions," AIAA Paper 2003-2657, July 2003.
- Roquemore, W. M., Vihinen, I., Hartrauft, J., and Mantis, P. M., "Trapped Vortex Combustor for Gas Turbine Engines," Annual Report to Strategic Environmental Research and Development Program, 1998.
- Hsu, K.-Y., Goss, L. P., and Roquemore, W. M., "Characteristics of a Trapped-Vortex Combustor," *Journal of Propulsion and Power*, Vol. 14, No. 1, 1998, p. 57.
- Sturgess, G. J., and Hsu, K.-Y., "Entrainment of Mainstream Flow in a Trapped-Vortex Combustor," AIAA Paper 97-0261, Jan. 1997.
- Roquemore, W. M., Shouse, D., Burrus, D., Johnson, A., Cooper, C., Duncan, B., Hsu, K.-Y., Katta, V. R., Sturgess, G. J., and Vihinen, I., "Trapped Vortex Combustor Concept for Gas Turbine Engines," AIAA Paper 2001-0483, Jan. 2001.
- Anthenian, R. A., Mantz, R. A., Roquemore, W. M., and Sturgess, G. J., "Experimental Results for a Novel, High Swirl, Ultra Compact Combustor for Gas Turbine Engines," *Western States Section Combustion Institute Meeting*, April 2001.
- Zelina, J., Ehret, J., Hancock, R. D., Shouse, D. T., Sturgess, G. J., and Roquemore, W. M., "Ultra-Compact Combustion Technology Using High Swirl to Enhance Burning Rate," AIAA Paper 2002-3725, June 2002.
- Mestre, A., and Benoit, A., "Combustion in Swirling Flow," *Proceedings of the Fourteenth International Symposium on Combustion*, Combustion Inst., Pittsburgh, PA, 1973, pp. 719-725.

³⁹Lewis, G. D., "Centrifugal-Force Effects on Combustion," *Proceedings of the Fourteenth International Symposium on Combustion*, Combustion Inst., Pittsburgh, PA, 1973, pp. 413–419.

⁴⁰Yonezawa, Y., Toh, H., Goto, S., and Obata, M., "Development of the Jet-Swirl High Loading Combustor," AIAA Paper 90-2451, July 1990.

⁴¹Zelina, J., Sturgess, G. J., Mansour, A., and Hancock, R. D., "Fuel Injection Design Optimization for an Ultra-Compact Combustor," International Society on Air Breathing Engines, Paper ISABE-2003-1089, Sept. 2003.

⁴²Sirignano, W. A., Delplanque, J. P., and Lui, F., "Selected Challenges in Jet and Rocket Engine Combustion Research," AIAA Paper 97-2701, July 1997.

⁴³Sirignano, W. A., and Liu, F., "Performance Increases for Gas-Turbine Engines Through Combustion Inside the Turbine," *Journal of Propulsion*

and Power, Vol. 15, No. 1, 1999, pp. 111–118.

⁴⁴Lui, F., and Sirignano, W. A., "Turbojet and Turbofan Engine Performance Increases Through Turbine Burners," AIAA Paper 2000-0741, Jan. 2000.

⁴⁵Eroglu, A., Dobbeling, K., Joos, F., and Brunner, P., "Vortex Generators in Lean-Premix Combustion," American Society of Mechanical Engineers, ASME 98-GT-487, June 1998.

⁴⁶Sturgess, G. J., "Turbine Burner for Near-Constant Temperature Cycle Gas Turbine Engine: Application to a Large Commercial Subsonic Transport Engine—A Progress Report," *Workshop on Inter-Turbine Burning Engines*, Air Force Research Lab. (AFRL), Cleveland, OH, Feb. 2003.

⁴⁷Daggett, D. L., "Water Misting and Injection of Commercial Aircraft Engines to Reduce Airport NO_x," NASA CR-2004-212957, March 2004.